Dimensionality and Modularity of Adaptive Variation: Divergence in Threespine Stickleback from Diverse Environments

Grant E. Haines,[1,*] Louis Moisan,[2] Alison M. Derry,[3] and Andrew P. Hendry[1]

1. Redpath Museum and Department of Biology, McGill University, Montreal, Quebec, Canada; 2. Department of Biology, Chemistry, and Geography, Université du Québec à Rimouski, Rimouski, Quebec, Canada; 3. Department of Biological Sciences, Université du Québec à Montréal, Montreal, Quebec, Canada

Submitted November 11, 2021; Accepted June 2, 2022; Electronically published December 21, 2022

Online enhancements: supplemental PDF.

ABSTRACT: Populations are subjected to diverse environmental conditions that affect fitness and induce evolutionary or plastic responses, resulting in phenotypic divergence. Some authors contend that such divergence is concentrated along a single major axis of trait covariance even if that axis does not lead populations directly toward a fitness optimum. Other authors argue that divergence can occur readily along many phenotype axes at the same time. We use populations of threespine stickleback (*Gasterosteus aculeatus*) from 14 lakes with contrasting ecological conditions to find some resolution along the continuum between these two extremes. Unlike many previous studies, we included several functional suites of traits (defensive, swimming, trophic) potentially subject to different sources of selection. We find that populations exhibit dimensionality of divergence that is high enough to preclude a history of constraint along a single axis—both for divergence in multivariate mean trait values and for the structure of trait covariances. Dimensionality varied among trait suites and were strongly influenced by the inclusion of specific traits, and integration of trait suites varied between populations. We leverage this variation into new insights about the process of divergence and suggest that similar analyses could increase understanding of other adaptive radiations.

Keywords: adaptation, dimensionality, integration, stickleback, radiation.

Introduction

Evolutionary biologists have long grappled with uncertainty regarding the dimensionality of evolutionary processes and patterns, parameters that can have important implications for rates and patterns of evolution as well as their constraints. Dimensionality can be understood as the number of axes that are required to describe a space, with a one-dimensional space being linear, a 2D space circular, a 3D space spherical, and so on, with "effective dimensionality" taking into account the shape of a space (Del Giudice 2021). Such dimensionality can be considered from the perspective of selection, phenotypic variation, or genetic variation—and any of these perspectives can focus within populations, on divergence among populations (i.e., the number of axes along which populations are able to differentiate from one another), or both. For instance, some authors argue that divergence is constrained mostly to the "genetic line of least resistance" ($\mathbf{g}_{max}$) or to the major axis of the genetic covariance matrix (the **G** matrix) and is thus relatively insensitive to the complexity and direction of selection (Schluter 1996; Hine et al. 2014). This constraint by $\mathbf{g}_{max}$ within populations would then result in a low-dimensional pattern of divergence (Schluter 1996). At the other extreme, authors contend that high-dimensional divergence is common and facilitated by a complex selection landscape acting on mostly uncorrelated traits with genetic variance somewhat evenly distributed across them (Mezey and Houle 2005; Nosil et al. 2009).

The dimensionality of evolution has important implications for rates of evolutionary change, directions in trait space along which adaptation is possible, and the number of niche spaces that can be filled, effectively determining the ability of a lineage to diversify under new selection pressures. As one example, if the dimensionality of the **G** matrix is low and correlated traits experience opposing selection pressures, the rate of evolution will be lower than if selection was focused in a single direction similar

* Corresponding author; email: grant.haines@mail.mcgill.ca.

ORCIDs: Haines, https://orcid.org/0000-0001-9085-0022; Moisan, https://orcid.org/0000-0002-6424-6750; Derry, https://orcid.org/0000-0001-5768-8027; Hendry, https://orcid.org/0000-0002-4807-6667.

 © 2022 The University of Chicago. All rights reserved. Published by The University of Chicago Press for The American Society of Naturalists. https://doi.org/10.1086/722483

to the main axis of genetic variation (Agrawal and Stinchcombe 2009). By contrast, high dimensionality of **G** could mean fewer constraints on the number of possible combinations of trait values and thus a greater number of ecological niches that can be rapidly filled by adaptation (Kirkpatrick 2009). Furthermore, multidimensionality of divergence promotes many-to-one mapping of multiple possible phenotypic "solutions" to selection that result in a common function and similar fitness (Alfaro et al. 2005; Wainwright et al. 2005; Wainwright 2007).

One way of conceptualizing and quantifying dimensionality is through the related concepts of modularity and integration. Modules are defined as groups of traits that are strongly correlated with each other but less strongly correlated with other groups of traits (Wagner and Altenberg 1996; Mitteroecker and Bookstein 2007; Wagner et al. 2007). Integration describes correlations between traits or within and between modules that limit their ability to vary independently, thus limiting the number of possible evolutionary trajectories without reorganization of the **G** matrix (Cheverud 1982; Arnold 1992; Wagner and Altenberg 1996; Mitteroecker and Bookstein 2007; Adams and Collyer 2016). A high degree of modularity (low integration of traits between modules) allows for more flexibility in evolutionary trajectories because of the relative independence of each trait group (Wagner and Altenberg 1996).

Most previous studies of dimensionality in evolution have focused, deliberately or not, on associations *within* one or two trait modules of functionally similar traits likely experiencing similar selection pressures. For example, Schluter (1996) focused mostly on traits related to trophic ecology in sticklebacks, Darwin's finches, sparrows, and deer mice. Hine et al. (2014) considered only cuticular hydrocarbons in *Drosophila*. Hansen and Houle (2008) used only different measurements of *Drosophila* wing shape. Kirkpatrick (2009) used fat and muscle traits for beef cattle, body shape measurements in the fish *Melanotaenia eachamensis*, wing shape measurements in *Drosophila*, lactation curves for dairy cows, and growth trajectories for mice. We suggest that these previous assessments of associations among functionally similar traits are likely to produce underestimates of evolutionary dimensionality on the whole organism (whether within or among populations) and overestimates of evolutionary constraints. Hence, our goal in the present study is to assess the dimensionality of divergence within and between hypothesized trait modules ("trait suites" hereafter unless referring to demonstrated covariance, in which case "module" is used) experiencing different selection pressures. We did so by considering multiple traits in each of three trait suites of different functional categories in phenotypically and environmentally divergent populations. We also focus our study on a radiation of numerous populations with a common ancestor to examine the divergence that has resulted from adaptation, differentiating it from the approach used by Schluter (1996). From this perspective, strong constraints imposed by $\mathbf{g}_{max}$ would result in diversification of populations along a common axis, and a more radial distribution of populations in phenotype space would indicate less genetically constrained divergence.

General Questions (Fig. 1)

1. What is the effective dimensionality of divergence among populations? This is not a question with a formal null expectation of effective dimensionality. Rather, it lends itself to comparative answers, for example that dimensionality is greater for one trait suite than for others. We also applied this question to each of the predefined functional trait suites as well as a single data set including all traits. If divergence is constrained to $\mathbf{g}_{max}$, then the primary axes of the trait suites will be more correlated with one another than if they are only weakly integrated and susceptible to multifarious selection.

2. To what extent do populations share common within-population correlation structures between trait modules? The more correlation structures between trait suites are shared among populations, the more their level of integration is conserved and divergence is constrained.

3. To what extent do functional trait suites covary as adaptive modules? Trait suites that constitute modules would strongly covary internally and be representative of axes of divergence that could be predicted on the basis of the environmental conditions imposing selection on the module, irrespective of pressures on other traits or trait suites.

4. To what extent are different environmental variables or groups of environmental variables associated with variation in all phenotypes and in the trait suites? Phenotypic divergence corresponding with environmental variation would indicate that the phenotypic variation is likely adaptive or shares common plastic responses and is only weakly constrained by correlations between trait suites.

Study System Background

Threespine stickleback (*Gasterosteus aculeatus*) is an excellent species for studying evolutionary dimensionality through the lens of modularity and integration. Stickleback are highly variable within and among populations, and freshwater populations are independently derived from ancestral marine populations (Bell and Foster 1994). Much of their trait variation is known to be correlated with environmental variables (Bell et al. 1993; Reimchen 1994; MacColl et al. 2013; McGee et al. 2013), and evidence from introduced populations strongly suggests

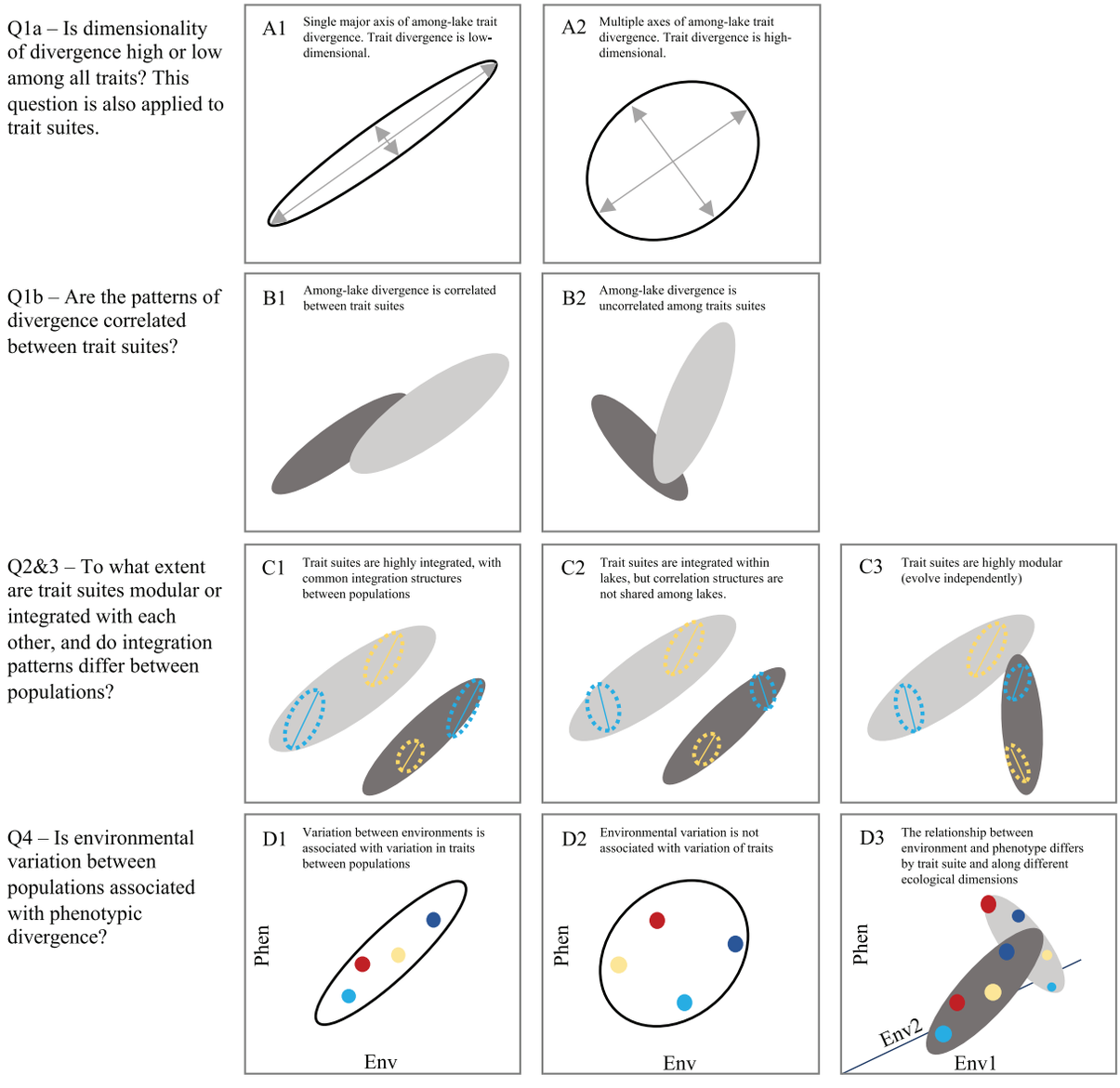

Figure 1: Conceptual diagrams illustrating the potential results of the questions addressed in this article. White ellipses represent total variation in phenotype between populations. Filled gray ellipses represent variation within trait suites between populations, open dashed ellipses represent populations, and solid circles represent population means. Lines bisecting population ellipses indicate the major axis of variation within that population for the trait suite in which it is shown. Panel axes, except in D1–D3, are arbitrary dimensions in a shared trait space, but trait suite ellipses are separated in some panels for illustrative purposes. For the tests that correspond with the panels, see table A1.

that adaptation is subject to multifarious and weakly constrained selection (Walker and Bell 2000; Aguirre and Bell 2012; Marques et al. 2018). Furthermore, stickleback divergence between habitat types (e.g., lake-stream [Lavin and McPhail 1993], benthic-limnetic [McPhail 1993], and marine-freshwater [Gelmond et al. 2009]) occurs in many traits, but the effective dimensionality that explains that divergence is largely unknown.

We collected stickleback and conducted environmental surveys for 14 lakes in the Cook Inlet region of southern Alaska. Stickleback populations in this region descend from anadromous populations from Cook Inlet (Bell et al. 1985). The region has a complex glaciation history (Reger et al. 2007; Kaufman et al. 2011) and is susceptible to earthquakes that can alter connectivity between habitats (Lescak et al. 2015), so the times at which the particular

populations in this study were established are unknown. However, recent molecular evidence from eight of the lakes included in our study supports this colonization scenario and minimal subsequent gene flow (Weber et al. 2021). Because freshwater stickleback populations are established from large anadromous populations rather than chance colonizations by a few individuals, bottlenecks and founder effects are not believed to be common, and none are evident in the molecular data (D. I. Bolnick, unpublished data). Additionally, stickleback population sizes in even small lakes can be on the order of tens to hundreds of thousands of individuals, limiting the effects of genetic drift (Reimchen 1990; Fisheries and Oceans Canada 2018). Occasional migration may occur between some sites and adjacent habitats, although this is generally not expected to prevent local adaptation (Haenel et al. 2021).

We divided trait measurements of the collected stickleback—a priori—into three functional suites (defensive, trophic, swimming) that could be under differing selection pressures. Although each trait could directly or indirectly influence multiple functions, we assigned the traits to the functions they influence most directly (details below). We also include landmark data describing body shape. Although body shape contributes to the functions of the other three trait suites and is therefore expected to be somewhat redundant (Berner et al. 2009; Bjærke et al. 2010), it also has very high intrinsic dimensionality and is commonly studied as a phenotypic response to environmental variation, making it particularly useful to contextualize results from the more function-specific trait suites. As a consequence, analyses for which the inclusion of shape would influence interpretation of functional traits suites were performed both with and without the inclusion of shape.

Our study focuses on lake environments diverse enough to preclude low-dimensional selection (Moodie and Reimchen 1976; Walker and Bell 2000; Spoljaric and Reimchen 2007). Nevertheless, the benthic-limnetic axis of divergence is likely to represent a major axis of phenotypic differentiation (Schluter and McPhail 1992; McPhail 1993; Willacker et al. 2010), is well documented between and within numerous fish species (Robinson and Wilson 1994; Jonsson and Jonsson 2001; Østbye et al. 2006; Friedman et al. 2020), and will be referred to when conveying some of the differences being described. This axis can be defined by benthic fish having a stouter and deeper body shape, a shortened head with a downturned jaw, and fewer short gill rakers. Limnetic fish, by contrast, have more elongate bodies and more numerous long gill rakers (Bentzen et al. 1984; McPhail 1993; Willacker et al. 2010). If divergence between these habitats is highly multidimensional, it will be distributed relatively evenly among multiple trait axes that are selected on by different environmental variables instead of being constrained primarily to a dominant axis of trait covariation.

Methods

Field Sampling

In May and June of 2018, we surveyed 14 lake populations of threespine stickleback from the Cook Inlet region of southwestern Alaska. The lakes surveyed were Corcoran, Finger, Long, Ruth, South Rolly, and Walby Lakes in the Matanuska-Susitna Valley and Echo, Engineer, G, Jean, Spirit, Tern, Wik, and Watson Lakes on the Kenai Peninsula (fig. 2; underlying data and code for this and subsequent figures can be found in the Dryad Digital Repository [https://doi.org/10.5061/dryad.v15dv41xw; Haines et al. 2022*b*] and Zenodo [https://doi.org/10.5281/zenodo.6355070; Haines et al. 2022*a*]). These populations were targeted in an effort to maximize morphological diversity along the benthic-limnetic axis of divergence while including some intermediate populations, using a combination of Willacker et al. (2010) and information from the Alaska Department of Fish and Game (personal communication). This design increased the likelihood that populations had sufficient phenotypic diversity to detect multidimensionality of divergence if it is present in wild populations more generally, and although some of these populations are close to one another geographically, they do not share surface connections that are plausible routes of dispersion. A variety of predatory fish are present in the lakes, especially salmonids and cottids, and the former are often stocked, but data were not sufficiently complete and current for inclusion in this study (Alaska Department of Fish and Game 2015).

Stickleback were captured in unbaited minnow traps and then killed with an overdose of clove oil, following the animal use protocol authorized by McGill University. Each fish was photographed immediately after death on 1-mm grid paper with a Nikon D800 (Finger, Walby, and 31 Long Lake fish) or a Canon PowerShot G11 (all others) and then preserved in 95% EtOH.

Linear Measurements and Meristic Traits

On their return to the laboratory, the following measurements were taken on fish by means of digital calipers with resolution to a hundredth of a millimeter: standard length (SL), body depth (BD), gape width (GW), buccal cavity length (BC), and the length of the pelvic and first and second dorsal spines (PS_L, $DS1_L$, and $DS2_L$, respectively; fig. 3). We also measured maximum width of the posterior process of the pterotic (PW), which articulates with the lateroanterior portion of the posttemporal, as an alternative to epaxial width. Following staining with

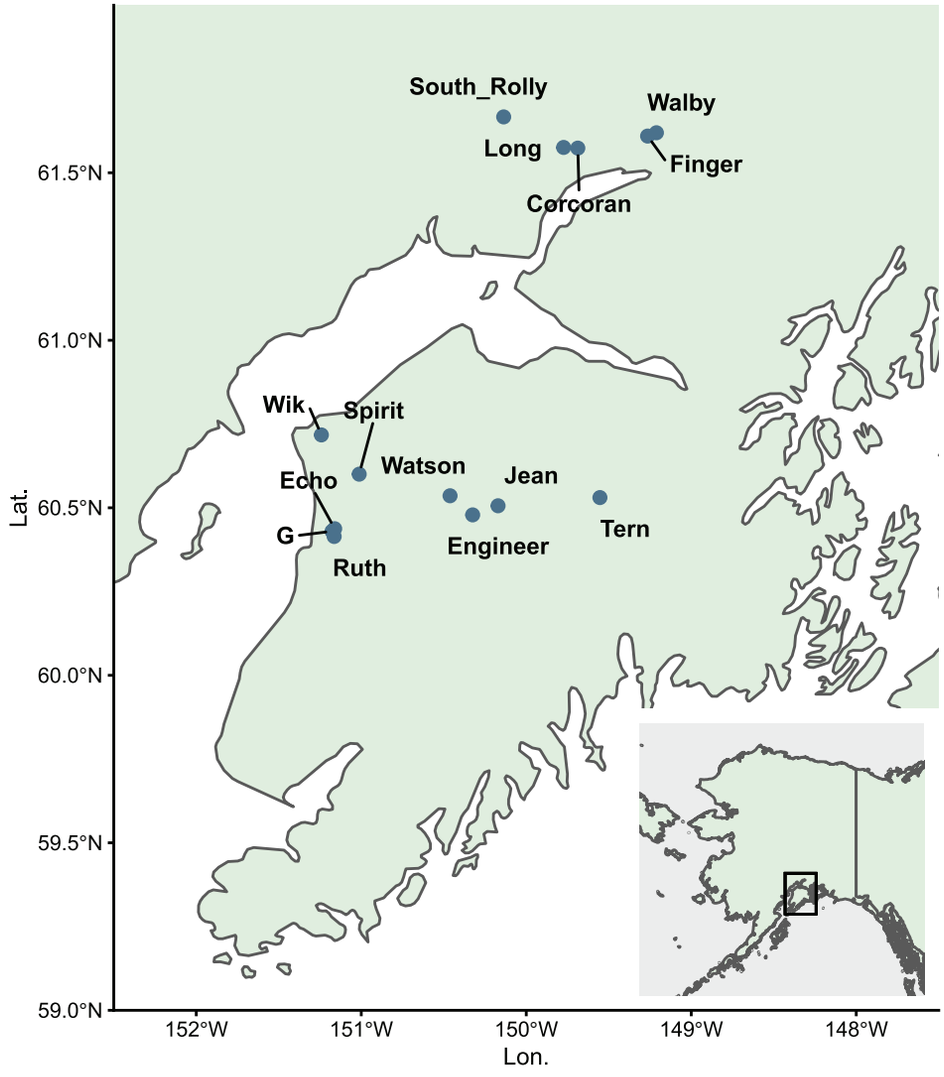

Figure 2: Locations of lakes in the Cook Inlet region of southern Alaska that were sampled for this study.

alizarin red-S dye as described by Springer and Johnson (2000), we counted lateral gill rakers of the first right branchial arch (GR) and the number of lateral plates (LP) on the both sides of the body (the average of the two sides was used for analysis). Using the digital photos, the following measurements were made in ImageJ (Rasband 1997–2018): caudal peduncle width (CP), upper jaw length (JL), snout length (SN), head length (HL), and eye diameter (ED; fig. 3).

Linear measurements were adjusted for allometry using the formula $M_{\text{std}} = M_{\text{O}}(\overline{\text{SL}}/\text{SL}_{\text{O}})^{b}$, where M_{O} and SL_{O} are the observed trait length and standard length, respectively; $\overline{\text{SL}}$ is the grand mean of all standard lengths (46.50 mm); and b is the slope of an ANCOVA of the form $M \sim \text{SL} + \text{lake}$ (Reist 1986; Hendry and Taylor 2004). GR, LP, and LP_{M} were not adjusted for allometry because all but two of our 792 fish had standard lengths <30 mm, the approximate size by which all gill rakers, lateral plates, and pelvic bones have formed (Bell 1981, 1987, 2001; Glazer et al. 2014). Spearman's rank correlations, with P values adjusted for multiple comparisons using the false detection rate (FDR) method (Benjamini and Hochberg 1995), confirmed that GR and LP were not correlated with SL in any lake.

Following Stuart et al. (2017), univariate measurements were then assigned to one of three trait suites (defense, trophic, swimming) on the basis of the type of selection they are expected to experience most directly based on the literature (table S1). Although some traits could be associated with more than one trait suite based on selection in the environment, each had to be assigned

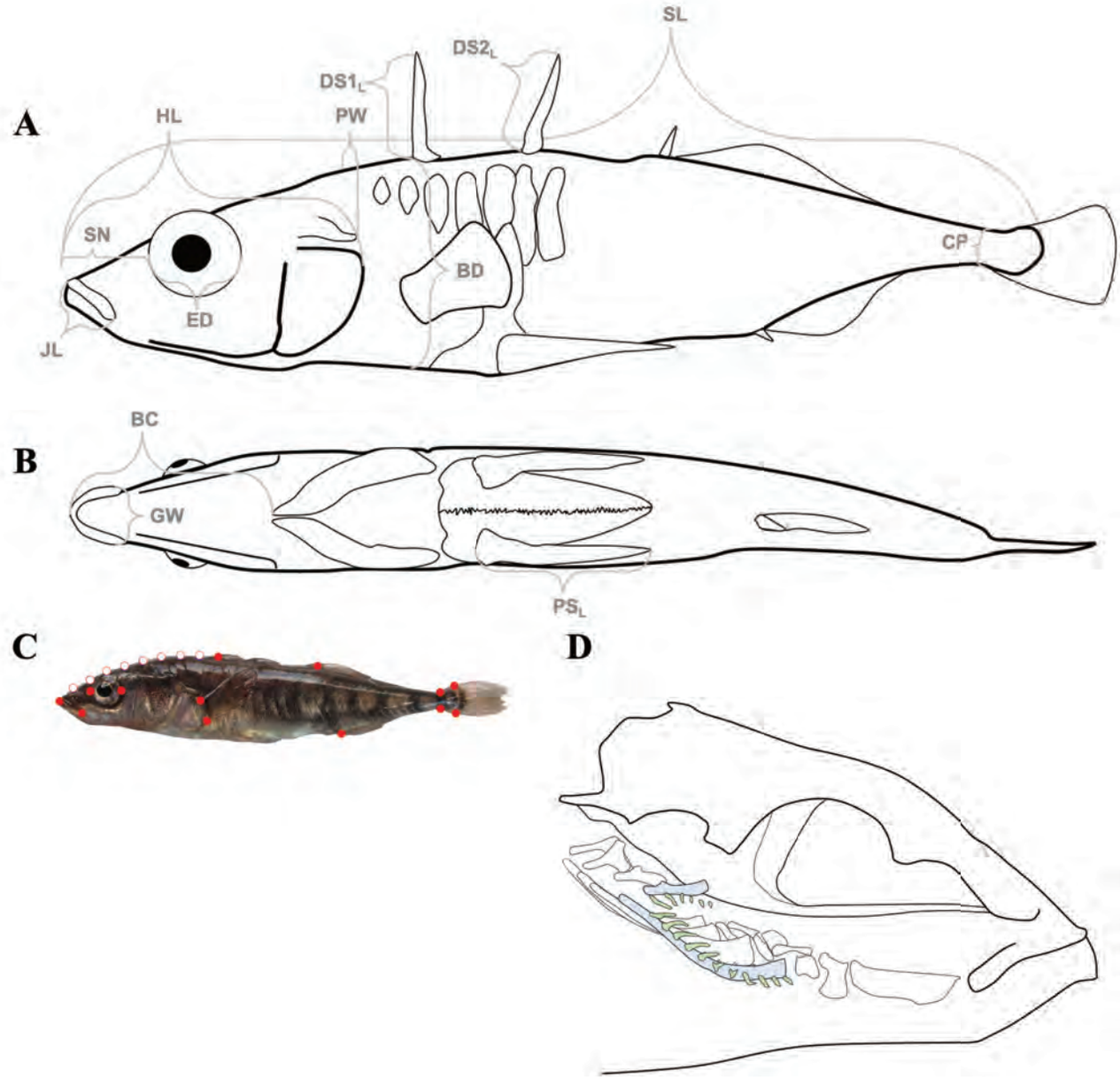

Figure 3: Univariate morphometric measurements from lateral (*A*) and ventral (*B*) views, geometric morphometric landmarks (closed) and semilandmarks (open; *C*), and the first branchial arch gill rakers (GR) that were counted (filled; *D*). Measurements shown are for upper jaw length (JL), snout length (SL), head length (HL), pterotic width (PW; width measured at widest point of pterotic posterior process), dorsal spine lengths ($DS1_L$ and $DS2_L$), standard length (BD), caudal peduncle width (CP), buccal cavity length (BC), gape width (GW), and pelvic spine length (PS_L). Medial rakers on the first right branchial arch were not counted (*C*). Only ossified lateral rakers were counted.

to a single trait suite for methodological reasons. Additionally, the tests of correlation between trait suites described below implicitly acknowledge the potential for functional overlap between trait suites. Missing values of traits—except GR, which had by far the lowest *N* of all traits recorded ($N_{GR} = 276$, or 34% of specimens)—were estimated using the regression formula of the most correlated trait with $r > 0.1$ within the same trait suite (numbers of individuals for which traits were thus estimated are provided in table S2). Units of traits were then standardized for multivariate analyses by transforming units into standard deviations of the total sample and centered about

zero (*Z* transformation). All data analyses were performed using the *R* statistical environment (ver. 4.0; R Core Team 2019).

Geometric Morphometrics

Body shape was quantified using landmark-based geometric morphometric methods, with 13 homologous anatomical landmarks placed from mouth to tail, to which eight semilandmarks were added to capture the curvature of the head from the tip of the snout to the first dorsal spine (fig. 3). Landmarks and semilandmarks were placed using tpsDig2 (ver. 2.31; Rohlf 2018). A Procrustes superimposition was performed on all specimens using the gpagen function in the R package geomorph (ver. 3.3; Adams and Otarola-Castillo 2013), with curves defined using minimum bending energy of the semilandmarks. Photographs of Long Lake specimens taken with the two different cameras were found to be significantly different with a Procrustes ANOVA, so landmark data for specimens photographed with the Nikon D800 were excluded from geometric morphometric analysis. Specimens for which the location of the landmark at the base of the first dorsal spine was uncertain were excluded, as this landmark was used to place the series of eight semilandmarks. Repeatability of shape was assessed to be 92% using variance ratios from Procrustes ANOVA, as described by Zelditch et al. (2012).

Shape is expected to be highly integrated with all three of the functional trait suites. This is because it is associated with defense from gape-limited predators (Reimchen 1991), with defense and swimming traits via its association with the fast-start response for predator avoidance (Taylor and McPhail 1986; Bergstrom 2002), and with swimming and trophic traits via the relationship between body depth and maneuverability in spatially complex foraging environments (Walker 1997; Feilich 2016). Additionally, linear measurements included in other trait suites, especially BD, ED, CP, and HL, describe aspects of shape, and thus these morphological traits are inextricably linked with the shape data. Because of the functional overlap with the other trait suites and because the shape data were available for two fewer lakes than the data describing the other trait suites, some subsequent analyses were conducted both including and excluding the shape data, with results provided in the supplemental PDF when they are not provided in the results section.

Limnological Conditions and Dietary Indicators

Lake physicochemical properties were measured in June of 2018 and June of 2019. These included total nitrogen (TN), total phosphorus (TP), chlorophyll-*a* (Chl-*a*), dissolved calcium (Ca), dissolved organic carbon (DOC), conductivity, and pH. These were all measured from epilimnetic water samples at the deepest point in each lake. Total surface area and maximum depth were obtained from previous Alaska Department of Fish and Game surveys. The proportion of littoral area (defined as an area <3 m deep) was calculated using Alaska Department of Fish and Game bathymetric maps when such maps were available. Zooplankton and benthic invertebrate community samples were collected using vertical Wisconsin net tows and D-frame kick net sampling, respectively, and were used to estimate the densities of a large limnetic grazer, *Daphnia* sp., in the pelagic zone and the densities of a dominant benthic macroinvertebrate family, gammarids, in the littoral zone of each lake. *Daphnia* sp. and gammarids are important components of the stickleback diet when they are present. Details of these field and laboratory methods, as well as a summary of expected adaptive responses to the environment, are provided in appendix A.

Statistical Analyses

Question 1: Dimensionality of Divergence and Correlations of Trait Suites. We examined the extent to which trait divergence among lake populations was multidimensional by first applying a linear discriminant analysis (LDA) including traits from all trait suites (MASS ver. 7.3; Venables and Ripley 2002; Ripley et al. 2020). The LDA determined the axis of greatest variation among lakes in relation to the variation within them. It is important here to note that unlike principal component analysis (PCA) axes, LDA axes are not orthogonal because LDA scales groups by their variances. For our rationale behind using LDAs, see appendix A. Because canonical variate analysis (CVA) and multivariate LDA are identical operations, this analysis was performed on shape data using the CVA function in the R package Morpho (ver. 2.8; Schlager 2017; Schlager et al. 2020), which provided an output that was more convenient for shape visualization but yielded the same results as lda in MASS (Ripley et al. 2020).

We next calculated the effective number of dimensions of multivariate divergence in all traits using several methods reviewed by Del Giudice (2021), shown in table 1. The third and fourth of these indices are very conservative and consistently overestimate effective dimensionality (D_e), respectively, but we include them for purposes of comparison to their usage elsewhere in the evolutionary biology literature. Because LDA is performed by singular value decomposition, we use the squares of the singular values (Ripley et al. 2020)—which are the canonical *F* statistics and used to calculate proportions of the trace explained by each LD axis—in place of eigenvalues in the D_e calculations. Despite our objections to the use of eigenvectors to

Table 1: Indices of effective dimensionality and variables used in their calculation

	Formula	Reference(s)	Note
D_e index:			
D_{n1}	$\prod_{i=1}^{n}\left(\frac{\lambda_i}{\sum_{i=1}^{n}\lambda_i}\right)^{-\lambda_i/\sum_{i=1}^{n}\lambda_i}$	Cangelosi and Goriely 2007; Roy and Vetterli 2007	…
D_{n2}	$\frac{\left(\sum_{i=1}^{n}\lambda_i\right)^2}{\sum_{i=1}^{n}\lambda_i^2}$	Pirkl et al. 2012	…
$D_{n\infty}$	$\sum_{i=1}^{n}\lambda_i/\lambda_1$	Kirkpatrick 2009	Excessively conservative
D_{nC}	$n-\frac{n^2}{\left(\sum_{i=1}^{n}\lambda_i\right)^2}\mathrm{var}(\lambda)$	Cheverud 2001	Overestimates D_e
	Description		
Variable:			
λ	Squared singular values of LD axes or eigenvalues for full data and population means		
λ_1	Squared singular value of LD1 or largest eigenvalue		
n	Number of squared singular values or eigenvalues		

Note: Details of these indices and their properties are described further and reviewed in Del Giudice (2021). All indices are bounded by a minimum of 1 and a maximum of n. LD = linear discriminant.

calculate divergence, we also calculated effective dimensionality of the population-level trait space using eigenvalues of population means as well as the trait space using eigenvalues of individual-level data for the purposes of comparison to other work and to place the D_e calculations from LDs in context. Dimensionality is a continuous variable, and so cutoffs for categorizing low, moderate, and high values are somewhat arbitrary. However, because these categories ease discussion, we regard low effective dimensionality as <2, moderate" as from 2 to 3, and high as >3. These values were chosen because the dimensionality of a circle projected onto a plane is 2 and the dimensionality of a sphere is 3, making their interpretation intuitive. For convenience, we will refer mostly to the D_{n1} effective dimensionality index unless otherwise noted. Because we are testing the extent to which this radiation aligns with two hypotheses along a continuum of dimensionality, there is no null hypothesis, and expectations are likely to vary by system and environmental complexity. We also note that effective dimensionality is not comparable to other methods of assessing dimensionality, such as that used by Mezey and Houle (2005).

Because gill rakers were counted in only approximately one-third of specimens, the above discriminant analysis for all traits was conducted with and without gill rakers. Additionally, this discriminant analysis excluded geometric morphometric landmark coordinates, both because landmarks excluded two lakes and because some components of shape share functions with other variables.

As with the data set of all traits, we conducted LDAs within defense, swimming, and trophic trait suites as well as shape and calculated the effective number of dimensions for each. We tested for correlations between the trait suites using pairwise Pearson correlations of the primary discriminant axes and Mantel tests of within-suite distance matrices of the specimens, calculated directly from standardized trait values. Each Mantel test used 500 iterations. Because the distribution of defensive traits violated the assumptions of Pearson's r, univariate and multivariate correlations including the defensive trait suite were performed using Spearman's rank correlation test in addition to the Pearson correlation test.

The effective dimensionality is limited by the number of traits included in each trait suite (e.g., the defensive trait suite, which includes five traits and cannot have an effective dimensionality greater than 5). Therefore, we implemented a rarefaction-like permutation procedure to visualize changes in effective dimensionality of divergence trait suites as traits are accumulated at random and compare suites of different numbers of traits. For details on this procedure see appendix A, and for results see appendix B and figure 7.

Question 2: Comparisons of Within-Lake Correlation Structures. We used two-block partial least squares correlation (2B-PLS) to test whether the trait suites were correlated within populations. This technique takes two data matrices from the same individuals—for example, our data for swimming

and defensive trait suites—and identifies the linear vectors through each data set that maximize covariation explained between the data sets (Rohlf and Corti 2000). We conducted 2B-PLS tests for all pairwise comparisons of trait suites. Each test yielded both a correlation coefficient (r_{PLS}) and a Z score (Adams et al. 2019). The Z score serves as an effect size of integration between the two blocks (here, trait suites) for each population and is comparable between 2B-PLS tests on populations with different sample sizes (Adams and Collyer 2016). We used these standardized effect sizes to compare the integration strength of trait suites between populations with pairwise two-sample Z-tests (Adams and Collyer 2016; Adams et al. 2019) and characterized the orientation of those differences by calculating the angle between vectors describing the most variance through data blocks between lakes. 2B-PLS tests and between-population Z-tests were performed using the two.b.pls and compare.pls functions, respectively, in the R package geomorph (Adams et al. 2019). Reported P values were adjusted for multiple comparisons using the FDR method (Benjamini and Hochberg 1995).

By way of a simple example, in a radiation of three populations (A, B, and C), we could conduct 2B-PLS tests between defensive traits and swimming traits in each population. The r_{PLS} statistic would give us the level of correlation between the defensive traits and swimming traits. Because r_{PLS} is sensitive to sample size, however, we compare the strength of correlations between trait suites using Z scores, which describe the strength of the effect relative to the null expectation of no association. If, after conducting pairwise Z-tests between populations, the comparisons between populations A and B yield a low effect size, but the A-C and B-C comparisons yield high effect sizes, then the strength of integration between defensive and swimming traits is similar between A and B but C differs from both. In this example radiation, then, the strength of the relationship between defense-associated and swimming-associated traits in population C diverged from that of the other two populations. Calculating vector angles between data blocks of the same trait suite for pairwise comparisons between lakes allowed us to compare orientation of integration structures, which are not considered in Z-tests for differences in strength of effects between lakes.

Because PLS methods are sensitive to both vector magnitude and orientation, our use of correlation matrices does produce different results in our 2B-PLS tests than use of covariance matrices would (and indeed we did use unstandardized geometric morphometric landmarks in these analyses, to the same effect). However, use of a correlation matrix for instances in which data do not all exist on the same scale, as is the case here, is recommended by Rohlf and Corti (2000) and even required for uses of 2B-PLS in which a block of morphological data is associated with a block of environmental data or other nonmorphological data related to niche occupation, as environmental data are rarely on the same scale (Corti et al. 1996; Fadda and Corti 1998; Felice et al. 2019).

Question 3: Evolutionary Modularity of Trait Suites. We tested the extent of modularity of trait suites, both within each population and across all populations, using the modularity.test function of geomorph, which tests whether the ratio of covariation between to within designated trait suites is less than if traits had been assigned to suites randomly (Adams 2016; Adams and Collyer 2019). When this test is applied to multiple trait suites simultaneously, the average of pairwise covariance ratios is used as a test statistic (Adams and Collyer 2019), which provides a better picture of overall modularity but provides less information about the independence of each trait suite. Consequently, these tests were executed in two ways, involving how partitions between trait suites were set. First, we performed the test after defining a partition separating a target trait suite from all other traits. These tests are referred to in the results section as "focused" tests. We then performed a test of modularity with all trait suites partitioned from one another, which we refer to in the results section as a "complete" test.

Because the measurements in the swimming trait suite were important components of shape, modularity tests were performed both with and without the inclusion of shape as a module to be sure that this redundancy did not alter results. All modularity tests were performed with 5,000 permutations. The P values reported for these tests are FDR adjusted for multiple comparisons.

Question 4: Responses to the Environment. We quantified environmental differences between lakes using PCA. This was first performed using physicochemical variables—pH, DOC, Ca, TN, TP, maximum depth, Chl-*a*, and surface area—for which complete data were available for all but two lakes (Echo and Ruth). This was followed by a PCA including both physicochemical variables and stickleback foraging-related ecological characteristics of the lakes, for which only a subset of lakes were surveyed. Both environmental PCAs used scaled environmental variables and thus were calculated using correlation matrices rather than covariance matrices. Stickleback foraging-related ecological characteristics included the areal proportion of littoral habitat (<3 m depth), *Daphnia* sp. abundance in the pelagic zone (number of individuals per liter), and gammarid abundance in the littoral zone (number of individuals per square meter). We also performed Spearman's correlations between each environmental variable and stickleback trait suite linear discriminant axes to determine the relationship between different environmental variables and axes of divergence (see app. B).

We subsequently executed 2B-PLS tests using normalized population-mean morphological variables as one block and environmental variables as the other. As with PCAs, we performed 2B-PLS tests twice using both physicochemical and full environmental data sets, the first including more lakes ($n = 12$) but the second including data related to foraging ($n = 9$). 2B-PLS is a balanced analysis that does not assume a direction of causality. It therefore may be a more accurate characterization of our system, in which eco-evo feedbacks potentially play a role, than another multivariate regression technique like redundancy analysis, which includes multivariate regression as its first step (Legendre et al. 2011). Additionally, 2B-PLS was more suited to our limited sample size because it uses a resampling procedure to generate the distribution for calculation of significance and effect size, and it is thus not limited by available degrees of freedom. Each 2B-PLS test yielded vectors through both the phenotype block and the environmental block, representing axes of greatest correlation between the two. The environmental data used in 2B-PLS tests are identical between tests, irrespective of trait suite phenotype. Because of this, the primary environmental vector angles between tests for different trait suites were calculated to quantify the divergence between environmental gradients along which divergence occurs.

Results

Axes of Divergence for All Traits and within Trait Suites

In the LDA including all defensive, trophic, and swimming traits, dimensionality was calculated to be high ($D_{n1} = 3.27$, $D_{n2} = 2.01$) when gill rakers were included ($N = 240$; table S3, 2). In this LDA, the primary axis explained 69.1% of the variance between populations, and the first three axis explained 87.3% of the variance. Standard length and pelvic spine length loaded most heavily on the first axis (table S4). The most important trait in the LDA was pelvic spine length, with a loading on LD1 four times the magnitude of the next largest coefficient, SL. Results were similar when gill rakers were excluded to increase the sample size. In this discriminant analysis ($N = 548$), dimensionality was only slightly lower ($D_{n1} = 3.09$, $D_{n2} = 1.90$). The first LD axis described 71.4% of interpopulation variance, and the first three axes described 88.0%.

An LDA of defensive traits showed that variation between populations was driven mostly by a single axis that accounted for 92.1% of this variation. Pelvic spine length (PS_L) was the variable most heavily loaded onto this axis, and it had a loading nearly eight times higher than $DS2_L$, the trait with the next highest loading. This result seems to be driven by the G Lake population, which was entirely lacking pelvic spines, and Echo Lake, which had only a single fish with pelvic spines. Dorsal spine lengths ($DS1_L$, $DS2_L$) drove most of the remaining variance in defensive traits between populations, and dimensionality of defensive trait divergence was low (tables 2, S5; figs. 4, S1). The low dimensionality driven by PS_L should not, however, be construed as demonstrative of a genetic constraint on divergence, as opposed to the consequence of particularly strong selection in G and Echo Lakes on an unconstrained trait. In fact, when these two lakes are removed from the analysis, still leaving 12 populations, the effective dimensionality of defensive trait divergence increases to $D_{n1} = 2.30$ or $D_{n2} = 1.71$.

Swimming traits, by contrast, had higher effective dimensionality of divergence than defensive traits, despite the swimming trait LDA including only three variables (SL, BD, and CP; tables 2, S6). LD1 of this discriminant function described 67.5% of variation between populations, with CP and BD being loaded approximately equally onto this axis. This placement of populations along this axis conformed to a priori expectations of the benthic-limnetic axis. More apparently limnetic populations, like G, Wik, and South Rolly Lakes, were assigned more negative values, and more benthic populations, like Watson and Tern Lakes, were assigned more positive values.

Trophic trait divergence was much more multidimensional than either swimming or defensive trait divergence, with effective dimensionality of $D_{n1} = 4.59$ and $D_{n2} = 3.48$ (table 2). This was also much higher than D_e calculated from eigenvalues of individual-level or population mean trait data. In the trophic trait suite, LD1 described only 44.5% of variation between populations, with PW, followed closely by HL and SN, being the variable most heavily loaded onto this axis (table S7).

Body shape was the most multidimensional of the trait suites, with high effective dimensionality of $D_{n1} = 7.16$ and $D_{n2} = 5.27$, albeit calculated from data with a much higher number of traits, with each landmark having an x and y coordinate (table 2). For shape, the first discriminant axis only described 35.2% of variation between populations, and five LD axes were required to explain at least 80%. The first axis here describes mostly body depth, but also angle of the head and the posterior extent of the dorsal fin. As with the swimming and to some extent the trophic suite, LD1 appears to reflect the benthic-limnetic continuum (figs. S1, S2).

Primary axes of all trait suite LDAs were significantly correlated with all other LD1s (fig. S3; table S8). The least correlated LD1s were those of the defensive and trophic trait suites (Pearson's $r = -0.21$, $P = .001$; Spearman's $\rho = -0.10$, $P = .121$). The most correlated trait suite LD1s were those of shape and swimming traits (Pearson's $r = 0.71$, $P < .001$; Spearman's $\rho = 0.72$, $P < .001$). Because of its intensely bimodal distribution, however, correlations between the defensive trait LD1 and the other trait

Table 2: Dimensionality of divergence in trait suites calculated using inertia of linear discriminants as well as eigenvalues of the full trait matrix and population means calculated from principal component analyses

	Defense			Trophic			Swimming			Shape			Total nonshape		
D_e type	LDA	Full matrix	Pop. means	LDA	Full matrix	Pop. means	LDA	Full matrix	Pop. means	LDA	Full matrix	Pop. means	LDA	Full matrix	Pop. means
D_{n1}	1.43	4.04	3.37	4.57	2.60	2.32	2.22	1.73	1.68	7.16	10.32	5.28	3.26	5.31	4.45
D_{n2}	1.18	3.63	3.00	3.47	1.75	1.66	1.90	1.39	1.36	5.27	6.63	4.23	2.01	2.99	2.99
$D_{n\infty}$	1.09	2.59	2.34	2.25	1.35	1.31	1.48	1.19	1.18	2.84	3.57	2.93	1.45	1.81	1.87
D_{nC}	1.75	4.62	4.34	6.70	4.43	4.17	2.42	1.85	1.80	9.91	36.66	33.07	7.54	11.64	11.65

Note: The final group of values represents all traits excluding shape, because (*a*) two populations were excluded from geometric morphometric analysis and (*b*) our swimming traits are largely redundant with our shape data. D_{n1} and D_{n2} are the D_e measures that are recommended for consideration, as $D_{n\infty}$ and D_{nC} systematically underestimate and overestimate dimensionality, respectively. LDA = linear discriminant analysis.

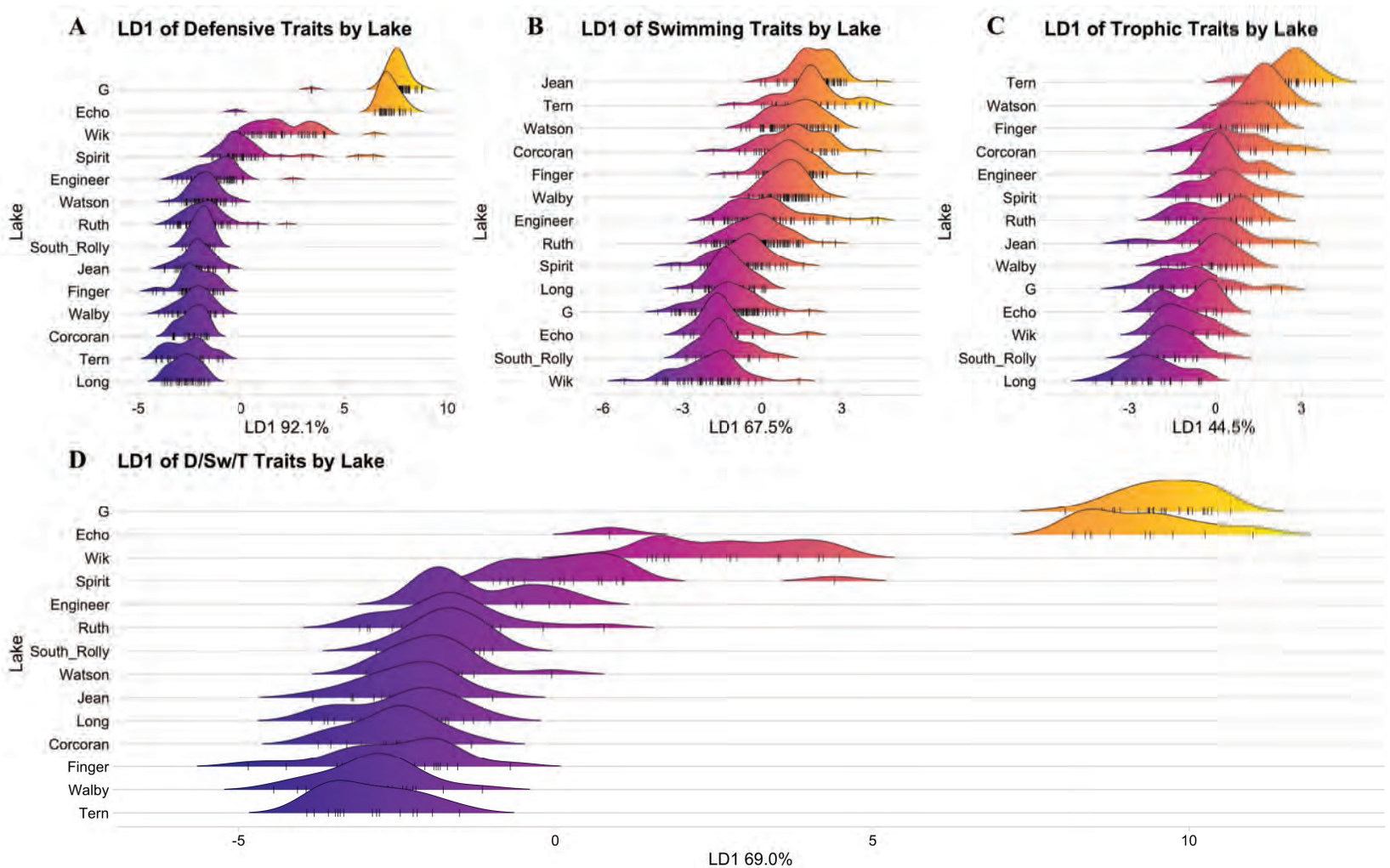

Figure 4: Distribution of individuals along primary linear discriminant axes for defensive, swimming, trophic, and combined traits. Positions of individual fish on each axis are indicated by the tick marks. Primary linear discriminant axes account for 92.1% (defense), 67.5% (swimming), 44.5% (trophic), and 69.0% (combined) of variances in their respective trait suites. Shape is excluded here because divergence is distributed evenly enough across canonical variate axes that visualizing only the first axis would contribute little to comprehension of results, and it is excluded from the combined discriminant score because variables in other trait suites (particularly the swimming suite) are redundant with important components of shape.

suites' primary LD axes should be viewed skeptically. Removing G and Echo Lakes, which included most of the individuals included in the smaller peak in defense LD1's distribution, reduced the strength of correlations between defense LD1 and the LD1 of other trait suites, including lowering the correlation with trophic LD1 to $r = -0.06$ ($P = .411$) and $\rho = 0.04$ ($P = .53$). Even after removing these populations, the apparent relationships between defensive and other trait suites remained idiosyncratic.

Mantel tests between full-dimensional data of all trait suites revealed that there was no significant multivariate correlation between the defensive trait suite and shape (Pearson's $r = 0.033$, $P = .106$; Spearman's $\rho = 0.037$, $P = .058$) and a relatively weak correlation between defensive and trophic trait suites (Pearson's $r = 0.077$, $P = .010$; Spearman's $\rho = 0.082$, $P = .002$; table S9). By far the strongest correlation shown in Mantel tests was between trophic and swimming traits (Pearson's $r = 0.788$, $P = .002$; Spearman's $\rho = 0.704$, $P = .002$), and all other multivariate correlations had correlation coefficients less than 0.13. To accommodate severe violations of the Pearson correlation's assumption of normality, we performed these tests using Spearman's rank correlation as well as Spearman's correlations. Both types of correlation tests yielded similar correlation coefficients. Although all trait suites did violate the assumption of multivariate normality as assessed using the Royston test for multivariate normality, this assumption was violated most severely by the defensive trait suite (Royston's $H = 308.1$, $P = 7.9 \times 10^{-65}$; when a partially plated individual from Spirit Lake was excluded, $H = 229.3$, $P = 6.9 \times 10^{-48}$).

Comparisons of Within-Lake Correlation Structures

Two-block PLS correlations between trait suites within populations show significant integration for each combination of trait suites in at least some lakes. Of these, the swimming × trophic suite tests show the most persistent trends ($r_{PLS} > 0.854$ in all cases, $Z_{range} = 2.35$–7.01, $P \leq .001$ in all lakes except Engineer, for which $P = .011$; table 3). The defensive trait suite and shape had by far the least consistent, and typically the weakest, relationship. Their r_{PLS} correlation coefficients ranged from 0.33 (Wik Lake, $Z = -1.71$, $P = .962$) to 0.79 (Echo Lake, $Z = 3.24$, $P = .006$; Long Lake, $Z = 0.99$, $P = .362$). The other pairs of trait suites mostly had clear integrative relationships, although the patterns of shared variation between defensive and trophic traits were also somewhat erratic between lakes.

Pairwise comparisons between lakes for the difference in PLS effect size in each pair of trait suites revealed several cases of clusters of populations that share similar integration strengths compared with other lakes, albeit typically with relatively moderate effect sizes, and none higher than $Z = 4.00$ (Wik × Tern, defense vs. shape; fig. S4). These groups do not clearly reflect populations' position along the benthic-limnetic axis, and in some cases lakes on opposite ends of the traditional benthic-limnetic axis share similar integration strengths. Watson and South Rolly Lakes, for instance, have quite similar strengths of integration between defensive and trophic traits despite Watson fish being very benthic and South Rolly fish being very limnetic.

More revealing were the patterns of relative orientation of PLS axes between lakes (fig. S5). In the swimming × trophic PLS test, axes of correlation between these trait suites were strikingly parallel across all lakes, with the angles between trophic suite axes never exceeding 26° between lakes and the angles between swimming suite axes never exceeding 24°. Integration structures between swimming and defensive traits or shape also resulted in quite parallel PLS axes for the swimming suite, although the orientations of the defensive trait and shape axes were much more muddled in these cases. The integration patterns between some trait suites, in contrast, sometimes clustered the lakes into more or less poorly defined groups, within which lakes shared similar PLS axis orientations and differed in similar ways from lakes in other clusters (fig. S5). However, the lakes comprising these clusters were not necessarily the same between integration structures. Additionally and surprisingly, as was the case with integration effect sizes, the lakes in the PLS axis orientation clusters did not map clearly onto the fairly obvious, but apparently superficial, benthic-limnetic continuum. One of the clusters in the defensive block defensive × trophic suite PLS angle matrix included Wik and G Lakes, both of which are extremely limnetic, but also Tern Lake, the most benthic of any of the lakes surveyed.

Modularity of Trait Suites

The complete modularity test showed a modular signal of modest strength in every population except Engineer. Modularity in Engineer Lake was only marginally insignificant and differed only slightly from other populations (table S10). However, the focused tests of modularity on individual trait suites revealed that the defensive trait suite exhibited moderate to high levels of independence in all lakes, with the effect being strongest in G, Wik, and Spirit Lakes and weakest in Long, Finger, and Engineer Lakes (table 4). When gill raker data are excluded from the trophic trait suite to increase sample size, the signal of modularity in defensive traits generally becomes even stronger, even exceeding $Z = -11$ in Wik and Spirit Lakes. This change in effect size may be a consequence of mutual association of defensive traits and GR on environmental variables, particularly Ca, pH, and conductivity (fig. B2). Modularity of trophic traits was not consistent between lakes and exhibited a significant, moderately sized signal in four lakes (Corcoran, G, Long, and Spirit).

Table 3: Statistical results of two-block partial least squares (PLS) correlation tests between trait suites within each lake

	Defense × swimming			Defense × trophic			Defense × shape			Swimming × trophic			Swimming × shape			Trophic × shape		
Lake	r_{PLS}	P	Z	r_{PLS}	P	Z	r_{PLS}	P	Z	r_{PLS}	P	Z	r_{PLS}	P	Z	r_{PLS}	P	Z
Corcoran	.719	.003	2.998**	.775	.021	2.399*	.584	.689	.077	.949	.001	6.072***	.619	.003	2.988**	.682	.056	1.715
Echo	.837	.002	4.905**	.868	.021	2.398*	.794	.006	3.236**	.986	.001	3.798***	.839	.002	4.222**	.949	.012	2.691*
Engineer	.612	.004	3.116**	.708	.427	.431	.502	.379	.737	.855	.011	2.361*	.662	.002	4.7**	.927	.041	1.765*
Finger	.768	.002	6.218**	.887	.007	4.128**	…	…	…	.972	.001	5.711***	…	…	…	.849	.012	3.679*
G	.462	.003	3.818**	.582	.034	2.436*	.337	.689	−.183	.91	.001	6.492***	.656	.002	6.929**	.767	.034	2.071*
Jean	.385	.129	1.216	.57	.429	.251	.552	.226	1.323	.912	.001	5.266***	.77	.002	6.285**	.926	.024	2.097*
Long	.871	.002	6.061**	.872	.007	4.677**	.795	.362	.991	.954	.001	6.827***	.681	.008	2.706**	.772	.035	1.908*
Ruth	.776	.002	7.265**	.711	.021	2.634*	.552	.08	2.162	.988	.001	6.338***	.686	.002	7.322**	.821	.055	1.545
South Rolly	.693	.003	3.384**	.751	.054	1.927	.487	.95	−1.099	.92	.001	4.319***	.74	.014	2.136*	.804	.024	2.659*
Spirit	.426	.048	2.238*	.443	.672	−.49	.384	.689	−.277	.899	.001	5.051***	.726	.002	5.326**	.716	.031	2.911*
Tern	.914	.002	5.496**	.836	.014	3.31*	.77	.006	3.704**	.971	.001	7.012***	.764	.002	4.83**	.67	.168	.968
Walby	.613	.004	4.264**	.533	.427	.38	…	…	…	.924	.001	5.722***	…	…	…	.776	.034	2.019*
Watson	.709	.002	6.2**	.702	.078	1.78	.511	.171	1.637	.955	.001	5.475***	.518	.012	2.499*	.682	.056	1.715
Wik	.434	.080	1.522	.632	.12	1.505	.333	.962	−1.711	.963	.001	5.414***	.688	.002	4.6**	.949	.012	2.691*

Note: P values are false detection rate adjusted for multiple comparisons. Negative Z scores indicate that trait suites are less integrated than would be expected given random associations of traits.

* $P < .05$.

** $P < .01$.

*** $P \leq .001$.

Table 4: Results of focused modularity tests for defense, swimming, and trophic trait suites when a single partition is set between the trait suite of interest and all other traits

	Defense				Swimming				Trophic			
Lake	CR	95% CI	*P*	*Z*	CR	95% CI	*P*	*Z*	CR	95% CI	*P*	*Z*
Corcoran	.959	.767–1.246	.002	−4.353**	1.15	1.071–1.194	.281	−.427	1.02	.915–1.128	.038	−3.73*
Echo	.984	.757–1.371	.005	−3.514**	1.171	1.13–1.229	.281	−.473	1.139	1.069–1.173	.806	.806
Engineer	.974	.767–1.34	.019	−2.166*	1.188	1.088–1.888	.399	−.32	1.024	.869–1.22	.124	−1.716
Finger	1.029	.872–1.142	.003	−2.901**	1.127	1.082–1.161	.243	−.543	1.095	1.054–1.133	.27	−.668
G	.701	.513–.969	.001	−7.636***	1.121	1.04–1.197	.243	−.302	1.017	.91–1.105	.038	−3.03*
Jean	.7	.589–1.082	.001	−4.394***	1.072	.926–1.188	.281	−.714	1.012	.856–1.176	.177	−1.234
Long	1.046	.905–1.135	.001	−2.993***	1.131	1.104–1.159	.243	−.726	1.056	.998–1.092	.038	−2.998*
Ruth	.927	.606–1.12	.001	−4.568***	1.179	1.167–1.207	.302	−.457	1.12	1.083–1.151	.683	.35
South Rolly	.931	.625–1.164	.001	−4.319***	1.115	.996–1.173	.243	−.815	1.079	.975–1.134	.177	−1.362
Spirit	.42	.401–.969	.001	−8.984***	1.067	.977–1.2	.243	−.657	.982	.782–1.118	.038	−3.042*
Tern	1.014	.904–1.115	.002	−4.197**	1.156	1.127–1.18	.281	−.557	1.071	1.009–1.114	.067	−2.69
Walby	.73	.533–1.089	.001	−5.574***	1.092	.945–1.137	.243	−.691	1.058	.93–1.123	.219	−.941
Watson	.87	.651–1.122	.001	−5.699***	1.144	1.066–1.211	.281	−.504	1.076	1.004–1.15	.216	−.985
Wik	.654	.443–1.13	.001	−8.787***	1.146	.992–1.18	.243	−.621	1.112	.956–1.153	.177	−1.226

Note: *P* values are false detection rate adjusted to account for multiple comparisons. CI = confidence interval; CR = covariance ratio.
* $p < .05$.
** $p < .01$.
*** $p \leq .001$.

Swimming traits were not modular in any population and had consistently weak effect sizes. That swimming traits are not modular was not surprising given the importance of swimming performance in both feeding and avoiding predation.

The inclusion of shape in a complete modularity test resulted in lower covariance ratios and slightly strengthened effect sizes of modularity (table S11). When shape was considered in a focused test of modularity, the signal of modularity was significant in all lakes and with strong effect sizes. Its inclusion in other focused tests also reduced the effect size of the modular signal in defensive traits, indicating the covariation between the defensive trait suite and some components of shape (table S12).

Responses to the Environment

The surveyed lakes are mostly of small to moderate size (minimum surface area = 2.7 ha, Ruth Lake [although Ruth was excluded from PCAs because of lack of Ca data]; maximum surface area = 135.7 ha, Finger Lake). However, these lakes exhibit a wide range of environmental characteristics. Lakes ranged from 2.1 (Corcoran) to 24.4 m (Wik) in maximum depth. All lakes had low to very low biomass of primary producers (maximum Chl-*a* = 3.30 μg L^{-1}, Finger Lake; minimum Chl-*a* = 0.42 μg L^{-1}, Wik Lake). The pH in the lakes ranged from circumneutral (pH = 6.6, Ruth Lake) to alkaline (pH = 8.8, Corcoran Lake), and Ca and conductivity were both very low in some lakes. The two lakes with the lowest Chl-*a*, Wik and G Lakes, also had the lowest Ca (1.3 and 0.6 mg L^{-1}, respectively) and conductivity (14.9 and 11.3 μS cm^{-1}, respectively). Jean Lake had the highest Ca (36.9 mg L^{-1}), and Finger Lake had the highest conductivity (239.0 μS cm^{-1}). Principal component biplots showing lakes and their relationships with environmental variables are presented in figure 5, with PC loadings and eigenvalues in tables S15 and S16. See appendix B for detailed results on foraging-related environmental variables.

2B-PLS regressions between trait suites and environmental variables did not reveal any significant correlations after *P* values were adjusted for multiple comparisons (fig. 6; table S15). However, physicochemical environmental variables alone were correlated with stickleback defensive and swimming trait suites at levels only slightly higher than the $P = .05$ threshold. While the trophic trait suite was not strongly correlated with physicochemical characteristics of the lakes, this association was strengthened substantially by the inclusion of ecological variables related to foraging (*Daphnia* sp. abundance, gammarid density, and percent littoral area), even though this reduced the number of lakes for which data was available to only eight lakes, and the correlation remained statistically insignificant. Axis loadings and singular values for all PLS tests are shown in tables S16–S19.

When the angles of the primary environmental vectors were calculated between 2B-PLS tests against different trait suites, angles involving the stickleback defensive trait suites were consistently largest. The defensive trait suite angles,

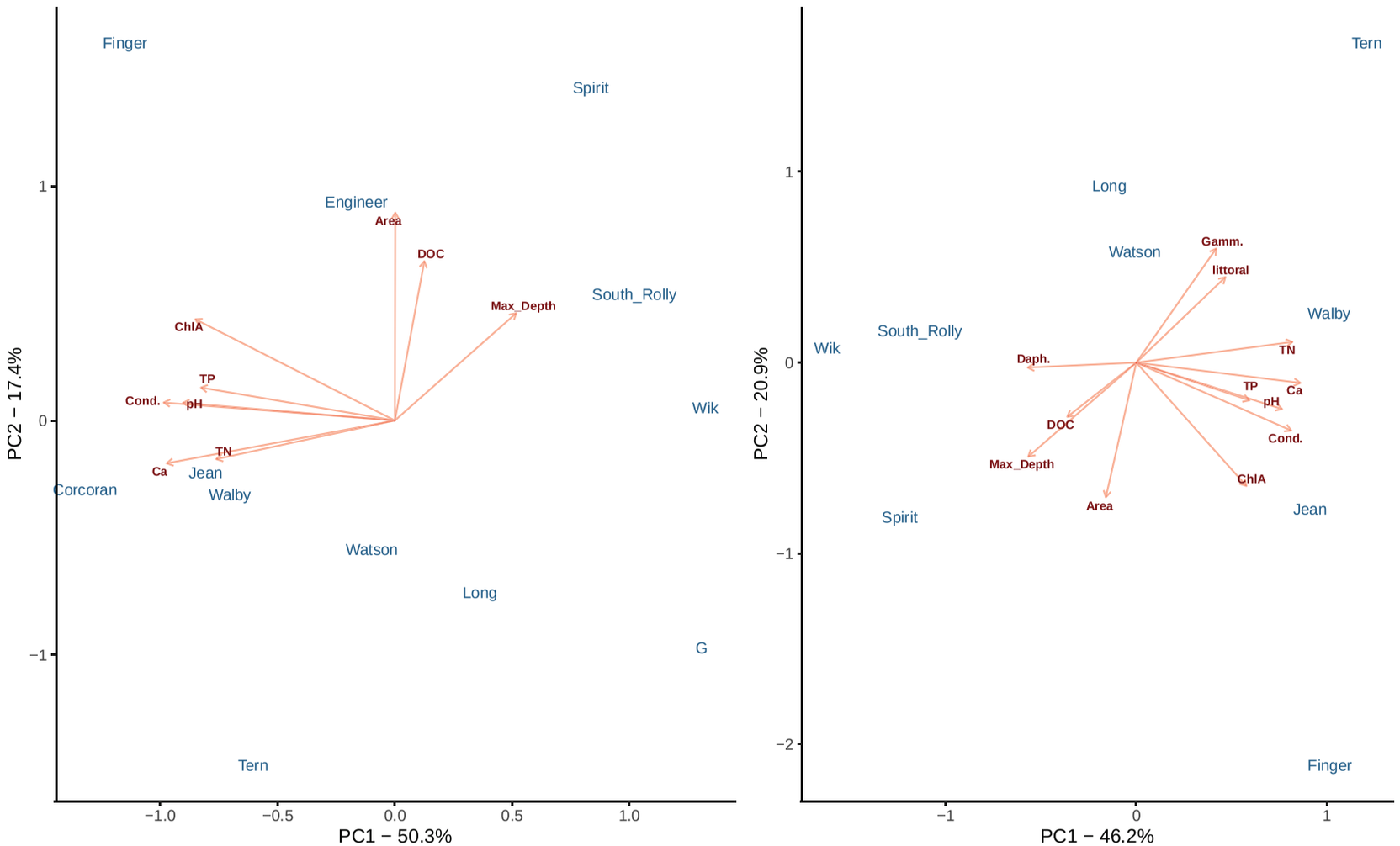

Figure 5: Principal component analysis (PCA) biplots of lakes and environmental variables. *A* shows physicochemical environmental variables. *B* shows a PCA biplot additionally including *Daphnia* abundance, gammarid abundance, and percent littoral area, all foraging-related environmental variables. Ruth Lake and Echo Lake are excluded from both panels because some environmental data were unavailable.

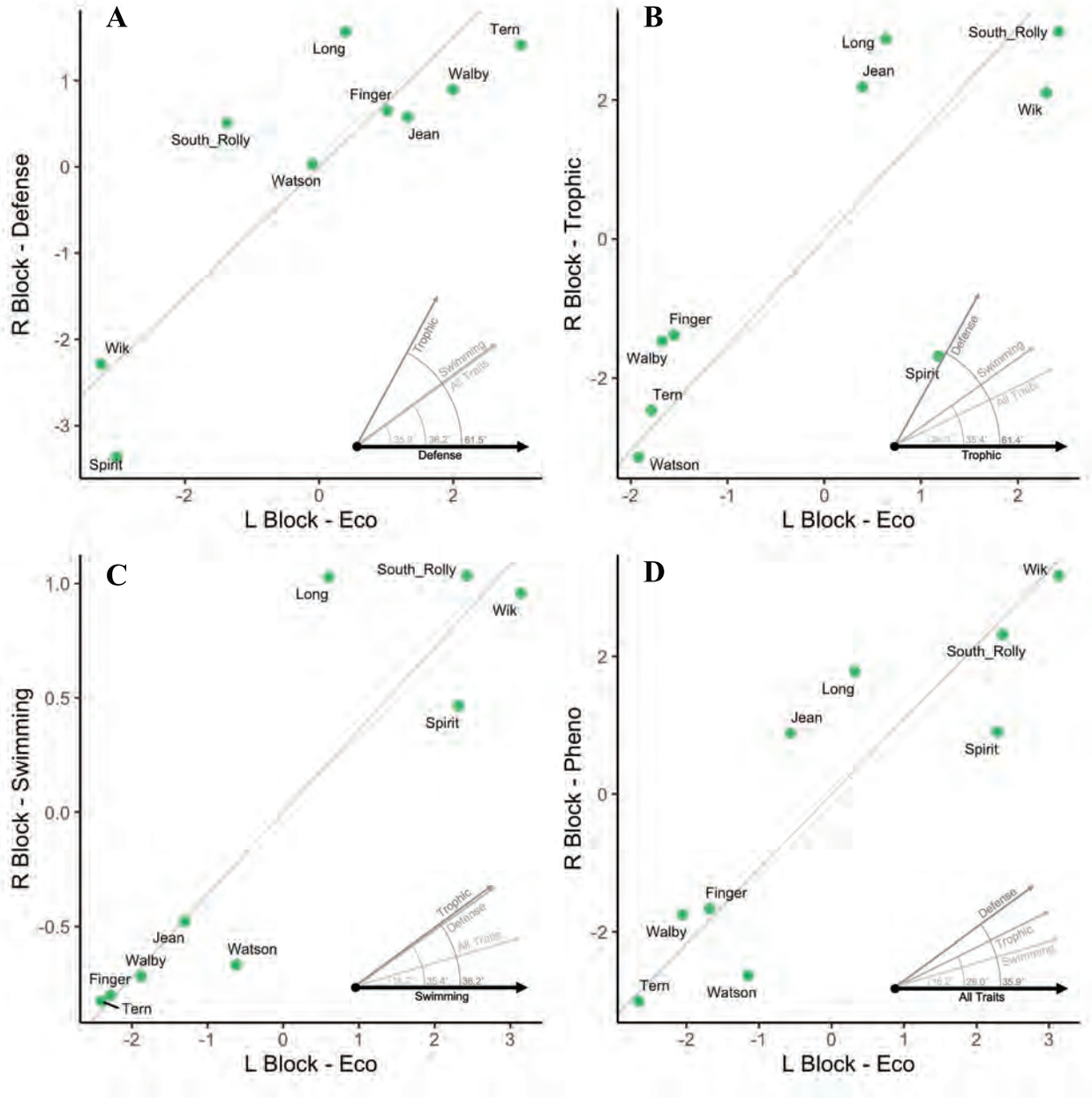

Figure 6: Plots of two-block partial least squares (PLS) axes of stickleback traits against all environmental characteristics. PLS axes are plotted by trait suite, with defensive traits in *A*, trophic traits in *B*, swimming traits in *C*, and traits from all three of those suites in *D*. Inset diagrams show angles of the plotted trait suite's primary vector through environmental space relative to the vectors of other trait groups through environmental space. The *x*-axes of all plots represents the major axis of phenotype-ecology covariation through the environmental data block, and the *y*-axes represent the same through the phenotypic data block.

especially the angles between the defensive trait suite environmental axis and the trophic trait suite environmental axis, indicate that the major axis of divergence in defensive traits among lakes occurs along an environmental gradient that is divergent from those of the other traits (fig. 6; table 5). These angles also widen greatly with the inclusion of foraging-related environmental data, further emphasizing the distinction between the axis of divergence in defensive traits and the more congruent trophic and swimming traits.

Although the populations of Echo, G, and Ruth Lakes are not connected by a viable route through which gene flow could take place, they are geographically proximate—all

Table 5: Angles of environmental vectors describing the axis of maximum covariance with traits in two-block partial least squares (PLS) correlation tests in relation to environmental vectors involving other trait suites

	All environmental variables			Physicochemical environmental variables		
	Defense	Swimming	All traits	Defense	Swimming	All traits
Defense	…	…	35.86	…	…	20.94
Swimming	36.18	…	16.2	27.36	…	9.91
Trophic	61.45	35.42	26.04	36.14	16.58	15.72

Note: Because diet-related environmental variables were available for only eight lakes, angles are shown from PLS tests including all environmental variables on the left and physicochemical variables only on the right. Angles of vectors are calculated in degrees, and the maximum possible angle was 90° because the sign of the vectors is arbitrary when the phenotype PLS blocks are not comparable between the tests.

within a few kilometers of one another. As a result, they have some environmental similarities that could be responsible for some phenotypic similarities. In particular, G and Echo both have very low Ca concentrations, and G, Echo, and Ruth have the three lowest pHs in our data set. Because Echo and Ruth were both missing certain data, the association between phenotype and physicochemical variables in our results is likely understated. These lakes are particularly close together, and this level of spatial autocorrelation appears to be an exception, rather than a rule, for our data. For example, Finger and Watson Lakes as well as Long and Corcoran Lakes are also relatively close geographically but do not exhibit the same degree of environmental similarity.

Discussion

Even on relatively short timescales, populations can often adapt in response to selection on several trait types simultaneously. This is the case for sticklebacks (Marques et al. 2018) and many other diverse taxa, including cichlid fishes (Hulsey et al. 2013; Hulsey et al. 2019), Galapagos finches (Grant and Grant 2006), *Anolis* lizards (Losos et al. 1997; Winchell et al. 2016), and mosquitofish (Langerhans 2018). However, because traits often covary, even when their functional relationships are not obvious or are indirect (Barrett et al. 2008; Bjærke et al. 2010), it has been difficult to establish whether populations diverge along a low-dimensional space (e.g., by following a genetic line of least resistance; Schluter 1996) or diverge in a higher-dimensional space as a consequence in response to multifarious selection on functionally disparate traits (Nosil et al. 2009). We hope that our study brings some clarity on these points to one exemplary adaptive radiation by showing that divergence in stickleback is not a unidimensional process but instead takes place along several axes both within and across trait suites under selection from distinct sources. This inflated dimensionality that we have demonstrated permits multiple possible evolutionary trajectories through phenotype space depending on the selection pressures experienced.

Opportunities for divergence are further influenced by the modularity and integration of trait groups under selection. For instance, although some within-lake patterns of integration between suites of traits are consistent across lakes, others vary considerably in both strength and direction between populations, permitting divergence that is not constrained to a common axis of covariance. Consistency and extent of trait suite modularity also varies by trait suite. The major axes of variation in the swimming and trophic trait suites also correspond to PLS axes of similar environmental variation. However, these morphological axes diverged from the environmental axis along which defensive traits varied, indicating potential trade-offs in which the optimum phenotypes of different trait suites diverge. We expect similar complexity to attend other classic study systems and are confident that analyses such as ours for those systems would bring increasingly general insights into the dimensionality of divergence.

The most multidimensional patterns of divergence were found in body shape data and in the trophic trait suite. For the defensive trait suite, by contrast, we found low dimensionality of divergence. Note, however, that this low dimensionality was due to LD1 being dominated by pelvic spine length, which was so divergent compared to other traits that it swamped divergence along other axes in the calculation of dimensionality. Importantly, although primary axes of divergence were strongly correlated between trait suites, trait suites were less strongly correlated with one another when they were considered as multivariate trait matrices. These patterns illustrate that lower-magnitude components of divergence may be more susceptible to selective pressures not shared between trait suites. This conclusion is also supported by the persistent signal of modularity between trait suites, even if its effect is relatively small overall.

Patterns of integration between trait suites often vary in strength and direction between populations, demonstrating that important axes of divergence exist not only in the trait values themselves but also in the ways that trait suites are related to one another. This variation could potentially influence how trait suites respond to the environment via both adaptation and plasticity. In addition to our conclusions about the dimensionality of divergence within and between trait suites, we established that the defensive trait suite was

the most independent of the trait suites we considered. This independence was evident from the inconsistent orientation of its axes of covariation with the other trait suites and from its high levels of modularity in all lakes when considered independently of shape. 2B-PLS tests of trait suites against environmental variables further showed that the environmental gradient along which defensive traits varied diverged in its orientation from the environmental gradients along which the other trait suites varied. In contrast, trophic and swimming traits varied much less independently than defensive traits, although some lakes did exhibit modularity in trophic phenotypes. The axes along which they were correlated with one another were also very similar among lakes.

Further Considerations for Future Work

Three notes of caution regarding dimensionality of divergence should accompany our findings.

1. The range of habitats that we have included, while ecologically diverse for lakes with stickleback populations, represent only a small subset of the range of habitats in which stickleback are found and consequently probably underestimate the magnitude, and likely the dimensionality, of divergence among stickleback populations more broadly. In addition to lake populations, there are anadromous marine and stream populations of threespine stickleback (Lavin and McPhail 1993; Bell and Foster 1994; Seebacher et al. 2016). Inclusion of either or both of these population types would likely have substantially increased the dimensionality of divergence generally, especially for the defensive trait suite when including anadromous populations and for the shape and swimming traits when including stream populations. In the former (anadromous) case, this is because threespine stickleback have three major lateral plate morphs—low, partial, and complete—and while low- and partial-plated morphs are common in fresh water, marine populations are typically made up almost entirely of completely plated morph (Hagen 1967; Bell and Foster 1994; Barrett et al. 2008). Of the stickleback represented in this study, there was only one single partially plated individual (from Spirit Lake), whereas the remainder were low plated, meaning that the fish we sampled only represent a small band of the possible variation in this trait and divergence in defensive traits was determined primarily by spine length in our data. In the latter case, populations of stickleback inhabiting streams typically have trophic adaptations suited to benthivory (Berner et al. 2008, 2009), and they have a deeper body shape that facilitates navigating the spatially heterogeneous flow regimes present in many streams (Hendry and Taylor 2004; Izen et al. 2016). Thus, the specificity of our study to threespine stickleback populations in lakes likely does not adequately represent the dimensionality of phenotypic divergence or the diversity of integration structures across the entire species.

2. Another important consideration is that our results seem to indicate that both effective dimensionality and variability in the orientation of covariance axes generally increase with the number of traits under consideration, a problem recognized by Schluter (1996). These observations are supported by our rarefaction-like analysis in appendix B and the increasing likelihood of vectors to be situated orthogonally to each other with increasing dimensionality of a space (Watanabe 2022), respectively. This effect may be intuitive—after all, our swimming trait suite, which is composed of only three traits, cannot possibly have more than three effective dimensions. Neither can the number of effective dimensions of divergence exceed one fewer than the number of populations under study. Nevertheless, the intrinsic dimensionality (i.e., the number of traits with variation; Del Giudice 2021) of divergence seems to not often be considered when authors assess whether an adaptive radiation is constrained to a line of least resistance (Schluter 1996). It is therefore important that researchers, when testing and making claims about the dimensionality of adaptation or divergence, measure broad ranges of traits of differing functions in populations of diverse habitat types unless the intention is to test a narrow question relating to patterns of adaptation in a particular suite of traits.

3. Finally, we advise other researchers to be conscious not just of the dimensionality of divergence in their systems but also of the magnitude of divergence. The measures of effective dimensionality that we have employed represent relative strengths of the vectors of divergence to one another but do not describe the extent to which they have diverged. In our case, although the populations we sampled are visibly divergent without measurement of any phenotypes, the large magnitude of the difference between the populations with pelvic spines and those without pelvic spines dwarfed other dimensions of divergence. As such, the inclusion of spine length actually reduced the effective dimensionality of phenotypic divergence, especially of the defensive trait suite, even when differences in other traits among populations were substantial (fig. 7). Consideration of magnitude is also necessary for divergence to be a useful metric of adaptive responses to the environment (Stuart et al. 2017; Runquist et al. 2020).

General Conclusions and Implications

Our findings suggest that divergence among populations is not typically constrained by the axis of greatest covariation, even within groups of traits that might be expected to respond to similar selection pressures. This conclusion is consistent with the known examples of highly divergent conspecific sympatric morphs even within a single habitat—especially among salmonids (Skúlason et al. 1989; Jónsson

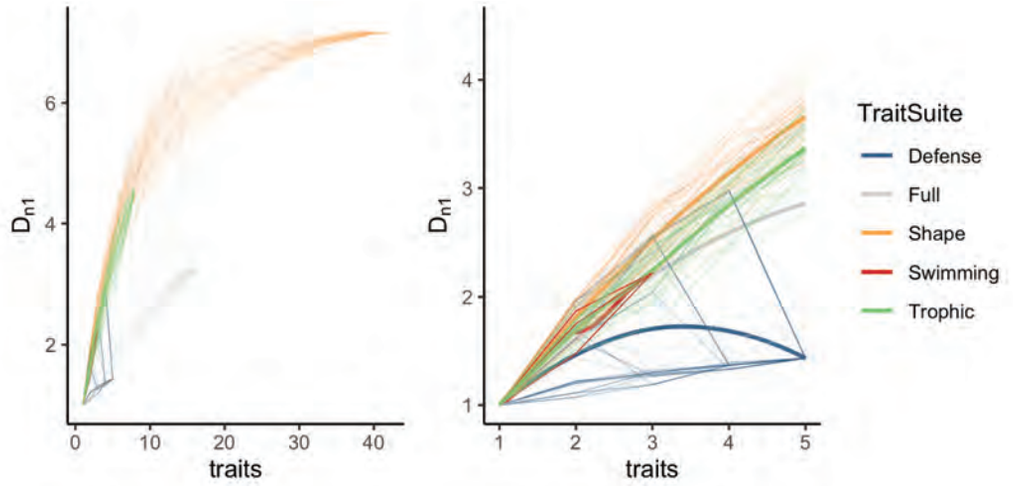

Figure 7: Effective dimensionality of divergence for each trait suite as well as the full nonshape phenotype data, with the inclusion of different numbers of traits. Thin lines represent 50 permutations of randomly sampling traits until all traits are included in the dimensionality calculation of linear discriminant analysis vectors. The left panel includes complete data from the permutation procedures, and the right panel shows only the first five traits in the permutations along with loess regressions showing the mean effective dimensionality for each trait suite at a given number of traits. See appendixes A and B for more on underlying methods and results.

and Skúlason 2000; Chaverie et al. 2016; Muir et al. 2016)—and is incompatible with a simple singly peaked or singly ridged fitness landscape. In practical terms, this means that populations under selection pressure should be able to approach fitness optima more quickly and more directly than if evolution is constrained to $\mathbf{g}_{max}$, perhaps in part because **G** matrices reorient so quickly in response to local selection that they do not function as a constraint, except over extremely short timescales. Some phenotypically diverse postglacial radiations—like some sticklebacks and the *Salvelinus* species—are particularly compelling in this respect because of the relatively short period of time available for the reorientation of $\mathbf{g}_{max}$. Yet other radiations also provide support for multiaxis divergence that is inconsistent with low-dimensional adaptation constrained by genetic covariances (Velasco and Herrel 2007; Hulsey et al. 2019; Levin et al. 2021). Recent work suggests that selection on developmental processes may be particularly powerful in their ability to rapidly change the shape of **G** and reorient $\mathbf{g}_{max}$ (Milocco and Salazar-Ciudad 2022). Further investigations into the role of plasticity—which Noble et al. (2019) have shown would be expected to facilitate low-dimensional divergence, in contrast to our results—is necessary for a more complete understanding of the role and limits of genetic constraint in divergence.

In closing, we note that our findings complicate the assessment of the repeatability and predictability of evolution in nature, one of the central themes of evolutionary biology (Bolnick et al. 2018). The possibility of adaptation in a high-dimensional space certainly makes predicting the evolutionary effect of an environmental condition in any particular instance difficult, even with high-quality data about multiple aspects of the environment and when the relatedness among populations is known (Stuart et al. 2017; Yong et al. 2020). This is not to say that predictions of the course of evolution are not worthwhile but rather that they should place greater emphasis on understanding the fitness landscape than the structure of the **G** matrix. This perspective will be particularly important in the context of rapid environmental change, when the ability to adapt along a number of axes may increase resilience, allowing a population to match the context of its specific habitat conditions (Reisch et al. 2015). Because the dimensionality of potential divergence is likely very taxon specific, further investigations into the genomic mechanisms and the role of plasticity through time in diverging populations will be necessary to develop useful predictive models for the evolution of species that are vulnerable, ecologically important, or important to human health.

Acknowledgments

This work was conducted under Alaska Department of Fish and Game permit SF2018-124 and Kenai National Wildlife Refuge permit 2018-Res-GHaines-6231 for stickleback collections and under Alaska Department of Fish and Game permit SF2018-001 for macroinvertebrate collections. The limnological research was funded by a Natural Sciences and Engineering Research Council of Canada (NSERC) Discovery grant to A.M.D., and other field work was supported

by an NSERC Discovery grant and Canada Research Chair (CRC) funding to A.P.H. We thank Stephanie Guernon and Maxime St Martin for zooplankton analyses and Nathan Juillet for macroinvertebrate analyses at Université du Québec à Montréal (UQAM). Many thanks to Mike Bell and Rob Massengill for their guidance and knowledge of local stickleback populations and to Blake Matthews for comments on the manuscript. We are also grateful to Junya Watanabe for comments on an early version of the manuscript regarding the dimensionality indices. Thanks also to Bailey Feddersen, Capucine Lechartre, Rebecca Pahulje, Ismail Ameen, and Greig Hospes for assistance with data collection and to Victor Frankel, Sarah Sanderson, Mariane Daneau-Lamoureux, and Michelle Packer for assistance in the field.

Statement of Authorship

G.E.H.: conceptualization, experimental design, data collection, data analysis, data visualization, writing—original draft and review and editing; L.M.: data collection, experimental design, writing—review and editing; A.M.D.: funding acquisition, data collection, supervision, experimental design, writing—review and editing; A.P.H.: funding acquisition, conceptualization, data collection, supervision, experimental design, writing—review and editing.

Data and Code Availability

The data associated with this article has been archived in the Dryad Digital Repository (https://doi.org/10.5061/dryad.v15dv41xw; Haines et al. 2022*b*). The R scripts used in the analysis, along with supplemental tables and figures, have been archived in Zenodo (https://doi.org/10.5281/zenodo.6355070 and https://doi.org/10.5281/zenodo.6355074, respectively; Haines et al. 2022*a*). Because of the large size and number of lateral photographs used for analysis, not all of them have been included, but a small number of them from each lake have been included in the Zenodo archive.

Literature Cited

Adams, D. C. 2016. Evaluating modularity in morphometric data: challenges with the RV coefficient and a new test measure. Methods in Ecology and Evolution 7:565–572.

Adams, D. C., and M. Collyer. 2019. Comparing the strength of modular signal, and evaluating alternative modular hypotheses, using covariance ratio effect sizes with morphometric data. Evolution 73:2352–2367.

———. 2016. On the comparison of the strength of morphological integration across morphometric datasets. Evolution 70:2623–2631.

Adams, D. C., M. Collyer, and A. Kaliontzopoulou. 2019. geomorph: geometric morphometric analysis of 2D/3D landmark data. Comprehensive R Archive Network.

Adams, D. C., and E. Otarola-Castillo. 2013. geomorph: an R package for the collection and analysis of geometric morphometric shape data. Methods in Ecology and Evolution 4:393–399.

Agrawal, A. F., and J. R. Stinchcombe. 2009. How much do genetic covariances alter the rate of adaptation? Proceedings of the Royal Society B 276:1183–1191.

Aguirre, W. E., and M. A. Bell. 2012. Twenty years of body shape evolution in a threespine stickleback population adapting to a lake environment. Biological Journal of the Linnean Society 105:817–831.

Alaska Department of Fish and Game. 2015. The Alaska Lake Database (ALDAT). Alaska Department of Fish and Game, Anchorage.

Alfaro, M. E., D. I. Bolnick, and P. C. Wainwright. 2005. Evolutionary consequences of many-to-one mapping of jaw morphology to mechanics in labrid fishes. American Naturalist 165:E140–154.

Arnold, S. J. 1992. Constraints on phenotypic evolution. American Naturalist 140:S85–S107.

Barrett, R. D. H., S. M. Rogers, and D. Schluter. 2008. Natural selection on a major armor gene in threespine stickleback. Science 322:255–257.

Bell, M. A. 1981. Lateral plate polymorphism and ontogeny of the complete plate morph of threespine sticklebacks (*Gasterosteus aculeatus*). Evolution 35:67–74.

———. 1987. Interacting evolutionary constraints in pelvic reduction of threespine sticklebacks, *Gasterosteus aculeatus* (Pisces, Gasterosteidae). Biological Journal of the Linnean Society 31:347–382.

———. 2001. Lateral plate evolution in the threespine stickleback: getting nowhere fast. Genetica 112:445–461.

Bell, M. A., and S. A. Foster. 1994. Introduction to the evolutionary biology of the threespine stickleback. Pages 1–27 *in* M. A. Bell and S. A. Foster, eds. The evolutionary biology of the threespine stickleback. Oxford University Press, New York.

Bell, M. A., R. C. Francis, and A. C. Havens. 1985. Pelvic reduction and its directional asymmetry in threespine sticklebacks from the Cook Inlet region, Alaska. Copeia 1985:437–444.

Bell, M. A., G. Ortí, J. A. Walker, and J. P. Koenings. 1993. Evolution of pelvic reduction in threespine stickleback fish: a test of competing hypotheses. Evolution 47:906–914.

Benjamini, Y., and Y. Hochberg. 1995. Controlling the false discovery rate: a practical and powerful approach to multiple testing. Journal of the Royal Statistical Society B 57:289–300.

Bentzen, P., M. S. Ridgway, and J. D. McPhail. 1984. Ecology and evolution of sympatric sticklebacks (*Gasterosteus*): spacial segregation and seasonal habitat shifts in the Enos Lake species pair. Canadian Journal of Zoology 62:2436–2439.

Bergstrom, C. A. 2002. Fast-start swimming performance and reduction in lateral plate number in threespine stickleback. Canadian Journal of Zoology 80:207–213.

Berner, D., D. C. Adams, A.-C. Grandchamp, and A. P. Hendry. 2008. Natural selection drives patterns of lake–stream divergence in stickleback foraging morphology. Journal of Evolutionary Biology 21:1653–1665.

Berner, D., A.-C. Grandchamp, and A. P. Hendry. 2009. Variable progress toward ecological speciation in parapatry: stickleback across eight lake-stream transitions. Evolution 63:1740–1753.

Bjærke, O., K. Østbye, H. M. Lampe, and L. A. Vøllestad. 2010. Covariation in shape and foraging behaviour in lateral plate morphs in the three-spined stickleback. Ecology of Freshwater Fish 19:249–256.

Bolnick, D. I., R. D. H. Barrett, K. B. Oke, D. J. Rennison, and Y. E. Stuart. 2018. (Non)parallel evolution. Annual Review of Ecology, Evolution, and Systematics 49:303–330.

Cangelosi, R., and A. Goriely. 2007. Component retention in principal component analysis with application to cDNA microarray data. Biology Direct 2:2.

Chaverie, L., W. J. Harford, K. L. Howland, J. Fitzsimons, A. M. Muir, C. C. Krueger, and W. M. Tonn. 2016. Multiple generalist morphs of Lake Trout: avoiding constraints on the evolution of intraspecific divergence? Ecology and Evolution 6:7727–7741.

Cheverud, J. M. 1982. Phenotypic, genetic, and environmental integration in the cranium. Evolution 36:499–516.

———. 2001. A simple correction for multiple comparisons in interval mapping genome scans. Heredity 87:52–58.

Corti, M., C. Fadda, S. Simson, and E. Nevo. 1996. Size and shape variation in the mandible of the fossorial rodent *Spalax ehrenbergi*: a Procrustes analysis of three dimensions. Pages 303–320 *in* L. F. Marcus, M. Corti, A. Loy, G. J. P. Naylor, and D. E. Slice, eds. Advances in morphometrics. Plenum, New York.

Del Giudice, M. 2021. Effective dimensionality: a tutorial. Multivariate Behavioral Research 56:527–542.

Fadda, C., and M. Corti. 1998. Geographic variation of *Arvicanthis* (Rodentia, Muridae) in the Nile Valley. Zeitschrift für Säugetierkunde 63:104–113.

Feilich, K. L. 2016. Correlated evolution of body and fin morphology in the cichlid fishes. Evolution 70:2247–2267.

Felice, R. N., J. A. Tobias, A. L. Pigot, and A. Goswami. 2019. Dietary niche and the evolution of cranial morphology in birds. Proceedings of the Royal Society B 286:20182577.

Fisheries and Oceans Canada. 2018. Recovery strategy for the Misty Lake sticklebacks (*Gasteosteus aculeatus*) in Canada. Species at Risk Act Recovery Strategy Series. Fisheries and Oceans Canada, Ottawa.

Friedman, S. T., S. A. Price, K. A. Corn, O. Larouche, C. M. Martinez, and P. C. Wainwright. 2020. Body shape diversification along the benthic-pelagic axis in marine fishes. Proceedings of the Royal Society B 287:20201053.

Gelmond, O., F. A. von Hippel, and M. S. Christy. 2009. Rapid ecological speciation in three-spined stickleback *Gasterosteus aculeatus* from Middleton Island, Alaska: the roles of selection and geographic isolation. Journal of Fish Biology 75:2037–2051.

Glazer, A. M., P. A. Cleves, P. A. Erickson, A. Y. Lam, and C. T. Miller. 2014. Parallel developmental genetic features underlie stickleback gill raker evolution. EvoDevo 5:19.

Grant, P. R., and B. R. Grant. 2006. Evolution of character displacement in Darwin's finches. Science 313:224–226.

Haenel, Q., K. B. Oke, T. G. Laurentino, A. P. Hendry, and D. Berner. 2021. Clinal genomic analysis reveals strong reproductive isolation across a steep habitat transition in stickleback fish. Nature Communications 12:4850.

Hagen, D. W. 1967. Isolating mechanisms in threespine sticklebacks (*Gasterosteus*). Journal of the Fisheries Research Board of Canada 24:1637–1692.

Haines, G. E., L. Moisan, A. M. Derry, and A. P. Hendry. 2022*a*. Code from: Dimensionality and modularity of adaptive variation: divergence in threespine stickleback from diverse environments. American Naturalist, Zenodo, https://doi.org/10.5281/zenodo.6355070.

———. 2022*b*. Data from: Dimensionality and modularity of adaptive variation: divergence in threespine stickleback from diverse environments. American Naturalist, Dryad Digital Repository, https://doi.org/10.5061/dryad.v15dv41xw.

Hansen, T. F., and D. Houle. 2008. Measuring and comparing evolvability and constraint in multivariate characters. Journal of Evolutionary Biology 21:1201–1219.

Hendry, A. P., and E. B. Taylor. 2004. How much of the variation in adaptive divergence can be explained by gene flow? an evaluation using lake-stream stickleback pairs. Evolution 58:2319–2331.

Hine, E., K. McGuigan, and M. W. Blows. 2014. Evolutionary constraints in high-dimensional trait sets. American Naturalist 184:119–131.

Hulsey, C. D., M. E. Alfaro, J. Zheng, A. Meyer, and R. Holzman. 2019. Pleiotropic jaw morphology links the evolution of mechanical modularity and functional feeding convergence in Lake Malawi cichlids. Proceedings of the Royal Society B 286:20182358.

Hulsey, C. D., R. J. Roberts, Y.-H. E. Loh, M. F. Rupp, and J. T. Streelman. 2013. Lake Malawi cichlid evolution along a benthic/limnetic axis. Ecology and Evolution 3:2262–2272.

Izen, R., Y. E. Stuart, Y. Jiang, and D. I. Bolnick. 2016. Coarse- and fine-grained phenotypic divergence among threespine stickleback from alternating lake and stream habitats. Evolutionary Ecology Research 17:437–457.

Jonsson, B., and N. Jonsson. 2001. Polymorphism and speciation in Arctic charr. Journal of Fish Biology 58:605–638.

Jónsson, B., and S. Skúlason. 2000. Polymorphic segregation in Arctic charr *Salvelinus alpinus* (L.) from Vatnshlídarvatn, a shallow Icelandic lake. Biological Journal of the Linnean Society 69:55–74.

Kaufman, D. S., N. E. Young, J. P. Briner, and W. F. Manley. 2011. Alaska palaeo-glacier atlas (version 2). Pages 427–445 *in* J. Ehlers, P. L. Gibbard, and P. D. Hughes, eds. Quaternary glaciations—extent and chronology: a closer look. Elsevier, Amsterdam.

Kirkpatrick, M. 2009. Patterns of quantitative genetic variation in multiple dimensions. Genetica 136:271–284.

Langerhans, R. B. 2018. Predictability and parallelism of multitrait adaptation. Journal of Heredity 109:59–70.

Lavin, P. A., and J. D. McPhail. 1993. Parapatric lake and stream sticklebacks on northern Vancouver Island: disjunct distribution or parallel evolution? Canadian Journal of Zoology 71:11–18.

Legendre, P., J. Oksanen, and C. J. F. ter Braak. 2011. Testing the significance of canonical axes in redundancy analysis. Methods in Ecology and Evolution 2:269–277.

Lescak, E. A., S. L. Bassham, J. Catchen, O. Gelmond, M. L. Sherbick, F. A. von Hippel, and W. A. Cresko. 2015. Evolution of stickleback in 50 years on earthquake-uplifted islands. Proceedings of the National Academy of Sciences of the USA 112:E7204–E7212.

Levin, B., E. Simonov, P. Franchini, N. Mugue, A. Golubtsov, and A. Meyer. 2021. Adaptive radiation and burst speciation of hillsteam cyprinid fish *Garra* in African river. bioRxiv, https://doi.org/10.1101/2021.05.04.442598.

Losos, J. B., K. I. Warheit, and T. W. Schoener. 1997. Adaptive differentiation following experimental island colonization in Anolis lizards. Nature 387:70–73.

MacColl, A. D. C., A. E. Nagar, and J. de Roij. 2013. The evolutionary ecology of dwarfism in three-spined sticklebacks. Journal of Animal Ecology 82:642–652.

Marques, D. A., F. C. Jones, F. D. Palma, D. M. Kingsley, and T. E. Reimchen. 2018. Experimental evidence for rapid genomic adaptation to a new niche in an adaptive radiation. Nature Ecology and Evolution 2:1128–1138.

McGee, M. D., D. Schluter, and P. C. Wainwright. 2013. Functional basis of ecological divergence in sympatric stickleback. BMC Evolutionary Biology 13:277.

McPhail, J. D. 1993. Ecology and evolution of sympatric sticklebacks (*Gasterosteus*): origin of the species pairs. Canadian Journal of Zoology 71:515–523.

Mezey, J. G., and D. Houle. 2005. The dimensionality of genetic variation for wing shape in *Drosophila melanogaster*. Evolution 59:1027–1038.

Milocco, L., and I. Salazar-Ciudad. 2022. Evolution of the *G* matrix under nonlinear genotype-phenotype maps. American Naturalist 199:420–435.

Mitteroecker, P., and F. Bookstein. 2007. The conceptual and statistical relationship between modularity and morphological integration. Systematic Biology 56:818–836.

Moodie, G. E. E., and T. E. Reimchen. 1976. Phenetic variation and habitat differences in Gasterosteus populations of the Queen Charlotte Islands. Systematic Zoology 25:49–61.

Muir, A. M., M. J. Hansen, C. R. Bronte, and C. C. Krueger. 2016. If Arctic charr *Salvelinus alpinus* is "the most diverse vertebrate", what is the lake charr *Salvelinus namaycush*? Fish and Fisheries 17:1194–1207.

Noble, D. W. A., R. Radersma, and T. Uller. 2019. Plastic responses to novel environments are biased toward phenotype dimensions with high additive genetic variation. Proceedings of the National Academy of Sciences of the USA 116:13452–13461.

Nosil, P., L. J. Harmon, and O. Seehausen. 2009. Ecological explanations for (incomplete) speciation. Trends in Ecology and Evolution 24:145–156.

Østbye, K., P.-A. Amundsen, L. Bernatchez, A. Klemetsen, R. Knudsen, R. Kristoffersen, T. F. Næsje, and K. Hindar. 2006. Parallel evolution of ecomorphological traits in the European whitefish *Coregonus lavaretus* (L.) species complex during postglacial times. Molecular Ecology 15:3983–4001.

Pirkl, R. J., K. A. Remley, and C. S. L. Patane. 2012. Reverberation chamber measurement correlation. IEEE Transactions on Electromagnetic Compatibility 54:533–545.

Rasband, W. S. 1997–2018. ImageJ. US National Institutes of Health, Bethesda, MD.

R Core Team. 2019. R: a language and environment for statistical computing. R Foundation for Statistical Computing, Vienna.

Reger, R. D., A. G. Sturman, E. E. Berg, and P. A. C. Burns. 2007. A guide to the late quaternary history of northern and western Kenai Peninsula, Alaska. Alaska Department of Natural Resources, Division of Geological and Geophysical Surveys, Anchorage.

Reimchen, T. E. 1990. Size-structured mortality in a threespine stickleback (*Gasterosteus aculeatus*)–cutthroat trout (*Oncorhynchus clarki*) community. Canadian Journal of Fisheries and Aquatic Sciences 47:1194–1205.

———. 1991. Trout foraging failures and the evolution of body size in stickleback. Copeia 1991:1098–1104.

———. 1994. Predators and morphological evolution in threespine stickleback. Pages 240–276 *in* M. A. Bell and S. A. Foster, eds. The evolutionary biology of the threespine stickleback. Oxford University Press, New York.

Reisch, R., T. Easter, C. A. Layman, and R. B. Langerhans. 2015. Rapid human-induced divergence of life-history strategies in Bahamian livebearing fishes (family Poeciliidae). Journal of Animal Ecology 84:1732–1743.

Reist, J. D. 1986. An empirical evaluation of coefficients used in residual and allometric adjustment of size covariation. Canadian Journal of Zoology 64:1363–1368.

Ripley, B., B. Venables, D. M. Bates, K. Hornik, A. Gebhardt, and D. Firth. 2020. Functions and datasets to support Venables and Ripley, Modern applied statistics with S (4th ed., 2002). Comprehensive R Archive Network.

Robinson, B. W., and D. S. Wilson. 1994. Character release and displacement in fishes: a neglected literature. American Naturalist 144:596–627.

Rohlf, F. J. 2018. tpsDIG2, digitize landmarks and outlines. State University of New York, Stony Brook.

Rohlf, F. J., and M. Corti. 2000. Use of two-block partial least-squares to study covariation in shape. Systematic Biology 49:740–753.

Roy, O., and M. Vetterli. 2007. The effective rank: a measure of effective dimensionality. Pages 606–610 *in* M. Domański and R. Stasiński, eds. 15th European Signal Processing Conference.

Runquist, R. D. B., A. J. Gorton, J. B. Yoder, N. J. Deacon, J. J. Grossman, S. Kothari, M. P. Lyons, S. N. Sheth, P. Tiffin, and D. A. Moeller. 2020. Context dependence of local adaptation to abiotic and biotic environments: a quantitative and qualitative synthesis. American Naturalist 195:412–431.

Schlager, S. 2017. Morpho and Rvcg—shape analysis in R: packages for geometric morphometrics, shape analysis and surface manipulations. Pages 217–256 *in* G. Zheng, S. Li, and G. Szekely, eds. Statistical shape and deformation analysis. Academic Press, London.

Schlager, S., G. Jefferis, and D. Ian. 2020. Morpho: calculations and visualisations related to geometric morphometrics. Comprehensive R Archive Network.

Schluter, D. 1996. Adaptive radiation along genetic lines of least resistance. Evolution 50:1766–1774.

Schluter, D., and J. D. McPhail. 1992. Ecological character displacement and speciation in sticklebacks. American Naturalist 140:85–108.

Seebacher, F., M. M. Webster, R. S. James, J. Tallis, and A. J. W. Ward. 2016. Morphological differences between habitats are associated with physiological and behavioural trade-offs in stickleback (*Gasterosteus aculeatus*). Royal Society Open Science 3:160316.

Skúlason, S., S. S. Snorrason, D. L. G. Noakes, M. M. Ferguson, and H. J. Malmquist. 1989. Segregation in spawning and early life history among polymorphic Arctic charr, *Salvelinus alpinus*, in Thingvallavatn, Iceland. Journal of Fish Biology 35:225–232.

Spoljaric, M. A., and T. E. Reimchen. 2007. 10 000 years later: evolution of body shape in Haida Gwaii three-spined stickleback. Journal of Fish Biology 70:1484–1503.

Springer, V. G., and G. D. Johnson. 2000. Use and advantages of ethanol solution of alizarin red S dye for staining bone in fishes. Copeia 2000:300–301.

Stuart, Y. E., T. Veen, J. N. Weber, D. Hanson, M. Ravinet, B. K. Lohman, C. J. Thompson, et al. 2017. Contrasting effects of environment and genetics generate a continuum of parallel evolution. Nature Ecology and Evolution 1:0158.

Taylor, E. B., and J. D. McPhail. 1986. Prolonged and burst swimming in anadromous and freshwater threespine stickleback, *Gasterosteus aculeatus*. Canadian Journal of Zoology 64:416–420.

Velasco, J. A., and A. Herrel. 2007. Ecomorphology of *Anolis* lizards of the Choco' region in Colombia and comparisons with Greater Antillean ecomorphs. Biological Journal of the Linnean Society 92:29–39.

Venables, W. N., and B. D. Ripley. 2002. Classification. *In* W. N. Venables and B. D. Ripley, eds. Modern applied statistics with S. Springer, New York.

Wagner, G. P., and L. Altenberg. 1996. Perspective: complex adaptations and the evolution of evolvability. Evolution 50:967–976.

Wagner, G. P., M. Pavlicev, and J. M. Cheverud. 2007. The road to modularity. Nature Reviews Genetics 8:921–931.

Wainwright, P. C. 2007. Functional versus morphological diversity in macroevolution. Annual Review of Ecology, Evolution, and Systematics 38:381–401.

Wainwright, P. C., M. E. Alfaro, D. I. Bolnick, and C. D. Hulsey. 2005. Many-to-one mapping of form to function: a general principle in organismal design? Integrative and Comparative Biology 45:256–262.

Walker, J. A. 1997. Ecological morphology of lacustrine threespine stickleback *Gasterosteus aculeatus* L. (Gasterosteidae) body shape. Biological Journal of the Linnean Society 61:3–50.

Walker, J. A., and M. A. Bell. 2000. Net evolutionary trajectories of body shape evolution within a microgeographic radiation of threespine sticklebacks (*Gasterosteus aculeatus*). Journal of Zoology 252:293–302.

Watanabe, J. 2022. Detecting (non)parallel evolution in multidimensional space: angles, correlations and eigenanalysis. Biology Letters 18:20210638.

Weber, J. N., N. C. Steinel, F. Peng, K. C. Shim, B. K. Lohman, L. Fuess, S. de Lisle, and D. I. Bolnick. 2021. Evolution of a costly immunity to cestode parasites is a pyrrhic victory. bioRxiv, https://doi.org/10.1101/2021.08.04.455160.

Willacker, J. J., F. A. von Hippel, P. R. Wilton, and K. M. Walton. 2010. Classification of the threespine stickleback along the benthic-limnetic axis. Biological Journal of the Linnean Society 101:595–608.

Winchell, K. M., R. G. Reynolds, S. R. Prado-Irwin, A. R. Puente-Rolón, and L. J. Revell. 2016. Phenotypic shifts in urban areas in the tropical lizard *Anolis cristatellus*. Evolution 70:1009–1022.

Yong, L., D. P., Croft, J. Troscianko, I. Ramnarine, and A. Wilson. 2020. Sensory-based quantification of male colour patterns in Trinidadian guppies reveals nonparallel phenotypic evolution across an ecological transition in multivariate trait space. bioRxiv, https://doi.org/10.1101/2020.11.23.394668.

Zelditch, M. L., D. L. Swiderski, and H. D. Sheets. 2012. General linear models. Pages 225–260 *in* Geometric morphometrics for biologists: a primer. Academic Press, Waltham, MA.

References Cited Only in the Online Enhancements

Anker, G. C. 1974. Morphology and kinetics of the head of the stickleback, *Gasterosteus aculeatus*. Transactions of the Zoological Society of London 32:311–416. https://doi.org/10.1111/j.1096-3642.1974.tb00030.x.

Bell, M. A., W. E. Aguirre, and N. J. Buck. 2004. Twelve years of contemporary armor evolution in a threespine stickleback population. Evolution 58:814–824. https://doi.org/10.1111/j.0014-3820.2004.tb00414.x.

Brooks, J. L. 1957. The systematics of North American *Daphnia*. Connecticut Academy of Arts and Sciences.

Brooks, J. L., and S. I. Dodson. 1965. The effect of a marine planktivore on lake plankton illustrates theory of size, competition, and predation. Science 150:28–35.

Caldecutt, W. J., and D. C. Adams. 1998. Morphometrics of trophic osteology in the threespine stickleback, *Gasterosteus aculeatus*. Copeia 4:827–838. https://doi.org/10.2307/1447330.

EPA (US Environmental Protection Agency). 1994. Method 200.7, revision 4.4: determination of metals and trace elements in water and wastes by inductively coupled plasma-atomic emission spectrometry. US Environmental Protection Agency, Cincinnati, OH.

Giles, N. 1983. The possible role of environmental calcium levels during the evolution of phenotypic diversity in Outer Hebriddean populations of the three-spined stickleback, *Gasterosteus aculeatus*. Journal of Zoology 199:535–544.

Griesbach, S. J., and R. H. Peters. 1991. The effects of analytical variations on estimates of phosphorus concentration in surface waters. Lake and Reservoir Management 7:97–106.

Haney, J. F., M. A. Aliberti, E. Allan, S. Allard, D. J. Bauer, W. Beagen, S. R. Bradt, et al. 2013. An image-based key to the zooplankton of North America, version 5.0. University of New Hampshire Center for Freshwater Biology, Durham. cfb.unh.edu/cfbkey/html/.

Hyman, J. M. 1983. Accurate monotonicity preserving cubic interpolation. SIAM Journal on Scientific and Statistical Computing 4:645–654.

Jones, C., K. M. Somers, B. Craig, and T. B. Reynoldson. 2007. Ontario benthos biomonitoring network: protocol manual. Queen's Printer for Ontario, Toronto.

Jones, J. R., M. A. Bell, J. A. Baker, and J. P. Koenings. 2003. General limnology of lakes near Cook Inlet, southcentral Alaska. Lake and Reservoir Management 19:141–149.

Klepaker, T., K. Østbye, and M. A. Bell. 2013. Regressive evolution of the pelvic complex in stickleback fishes: a study of convergent evolution. Evolutionary Ecology Research 15:413–435.

Klepaker, T., K. Østbye, R. Spence, M. Warren, M. Przybylski, and C. Smith. 2016. Selective agents in the adaptive radiation of Hebridean sticklebacks. Evolutionary Ecology Research 17:243–262.

Lipka, C. G., J. L. Gates, and S. K. Simons. 2020. Sport fisheries of the Northern Kenai Peninsula Management Area, 2016–2018, with overview for 2019. Fishery Management Report. Alaska Department of Fish and Game, Anchorage.

Mack, H. R., J. D. Conroy, K. A. Blocksom, R. A. Stein, and S. A. Ludsin. 2012. A comparative analysis of zooplankton field collection and sample enumeration methods. Limnology and Oceanography Methods 10:41–53.

Massengill, R., R. N. Begich, and K. Dunker. 2020. Operational plan: Kenai Peninsula nonnative fish control, monitoring, and native fish restoration. Regional Operation Plan. Alaska Department of Fish and Game, Anchorage.

McGee, M. D., and P. C. Wainwright. 2013. Convergent evolution as a generator of phenotypic diversity in threespine stickleback. Evolution 64:1204–1208. https://doi.org/10.1111/j.1558-5646.2012.01839.x.

Merritt, R. W., K. W. Cummins, and M. B. Berg, eds. 2008. Introduction to the aquatic insects of North America. Kendall Hunt, Dubuque, IA.

Moisan, J. 2010. Guide d'identification des principaux macroinvertébrés benthiques d'eau douce du Québec, 2010—Surveillance volontaire des cours d'eau peu profonds. Bibliothèque et archives nationales du Québec (CA): Direction du suivi de l'état de l'environnement, ministère du Développement durable, de l'Environnement et des Parcs.

Palkovacs, E. P., and D. M. Post. 2008. Eco-evolutionary interactions between predators and prey: can predator-induced changes to prey

communities feed back to shape predator foraging traits? Evolutionary Ecology Research 10:699–720.

———. 2009. Experimental evidence that phenotypic divergence in predators drives community divergence in prey. Ecology 90:300–305.

Patton, C. J., and J. R. Kryskalla. 2003. Methods of analysis by the U.S. Geological Survey National Water Quality Laboratory: evaluation of alkaline persulfate digestion as an alternative to Kjeldahl digestion for determination of total and dissolved nitrogen and phosphorus in water. Water-Resources Investigations Report. US Department of the Interior, US Geological Survey.

Reimchen, T. E. 1983. Structural relationships between spines and lateral plates in threespine stickleback (*Gasterosteus aculeatus*). Evolution 37:931–946. https://doi.org/10.2307/2408408.

———. 2000. Predator handling failures of lateral plate morphs in *Gasterosteus aculeatus*: functional implications for the ancestral plate condition. Behaviour 137:1081–1096. https://doi.org/10.1163/156853900502448.

Reimchen, T. E., C. Bergstrom, and P. Nosil. 2013. Natural selection and the adaptive radiation of Haida Gwaii stickleback. Evolutionary Ecology Research 15:241–269.

Reimchen, T. E., and P. Nosil. 2006. Replicated ecological landscapes and the evolution of morphological diversity among *Gasterosteus* populations from an archipelago on the west coast of Canada. Canadian Journal of Zoology 84:643–654. https://doi.org/10.1139/Z06-036.

Reimchen, T. E., D. Steeves, and C. A. Bergstrom. 2016. Sex matters for defense and trophic traits of threespine stickleback. Evolutionary Ecology Research 17:459–485.

Sartory, D. P., and J. U. Grobbelaar. 1984. Extraction of chlorophyll *a* from freshwater phytoplankton for spectrophotometric analysis. Hydrobiologia 114:177–187.

Schmid, D. W., M. D. McGee, R. J. Best, O. Seehausen, and B. Matthews. 2019. Rapid divergence of predator functional traits affects prey composition in aquatic communities. American Naturalist 193:331–345.

Taylor, D. J., and P. D. N. Hebert. 1993. Cryptic intercontinental hybridization in *Daphnia* (Crustacea): the ghost of introductions past. Proceedings of the Royal Society B 254:163–168.

Thorp, J. H., and A. P. Covich, eds. 2010. Ecology and classification of North American freshwater invertebrates. Academic Press, Burlington, MA.

Wintermans, J. F., and A. de Mots. 1965. Spectrophotometric characteristics of chlorophylls a and b and their pheophytins in ethanol. Biochimica et Biophysica Acta 109:448–453.

Witty, L. M. 2004. Practical guide to identifying freshwater crustacean zooplankton. 2nd ed. Department of Biology, Laurentian University Cooperative Freshwater Ecology Unit.

Associate Editor: Roi Holzman
Editor: Jennifer A. Lau

A bird's-eye view of Tern Lake in Church National Forest, on Alaska's Kenai Peninsula. Photo by Andrew P. Hendry.